Boron isotopic composition of olivine-hosted melt inclusions from Gorgona komatiites, Colombia: new evidence supporting wet komatiite origin

Andrey A. Gurenko[1,2]*, Vadim S. Kamenetsky[3]

[1] Woods Hole Oceanographic Institution, Geology & Geophysics, Woods Hole, MA 02543, USA

[2] Centre de Recherches Pétrographiques et Géochimiques, CNRS-Nancy Université, BP 20, F-54501 Vandoeuvre-lès-Nancy, France

[3] School of Earth Sciences and Centre for Ore Deposit Research, University of Tasmania, Australia

Revised version submitted to

Earth and Planetary Science Letters

Components:

Abstract: 316 words; 2,064 characters with spaces;

Main text: 6,473 words; 40,573 characters with spaces;

5 figures, 2 tables;

List of references includes 91 citations.

On-line supplementary Material: Analytical Methods, 2 figures

*** Corresponding author and present address:**

Andrey A. Gurenko, Centre de Recherches Pétrographiques et Géochimiques, 15, rue Notre-Dame des Pauvres, B.P. 20, 54501 Vandoeuvre-lès-Nancy, France. Phone: +33 (0)3 83 59 48 75, Fax: +33 (0)3 83 51 17 98, E-mail: agurenko@crpg.cnrs-nancy.fr

Abstract – A fundamental question in the genesis of komatiites is whether these rocks originate from partial melting of dry and hot mantle, 400–500°C hotter than typical sources of MORB and OIB magmas, or if they were produced by hydrous melting of the source at much lower temperatures, similar or only moderately higher than those known today. Gorgona Island, Colombia, is a unique place where Phanerozoic komatiites occur and whose origin is directly connected to the formation of the Caribbean Large Igneous Province. The genesis of Gorgona komatiites remains controversial, mostly because of the uncertain origin of volatile components which they appear to contain. These volatiles could equally result from shallow level magma contamination, melting of a "damp" mantle or fluid-induced partial melting of the source due to devolatilization of the ancient subducting plate. We have analyzed boron isotopes of olivine-hosted melt inclusions from the Gorgona komatiites. These inclusions are characterized by relatively high contents of volatile components and boron (0.2–1.0 wt.% H_2O, 0.05–0.08 wt.% S, 0.02–0.03 wt.% Cl, 0.6–2.0 µg/g B), displaying positive anomalies in the overall depleted, primitive mantle (PM) normalized trace element and REE spectra ($[La/Sm]_n$ = 0.16–0.35; $[H_2O/Nb]_n$ = 8–44; $[Cl/Nb]_n$ = 27–68; $[B/Nb]_n$ = 9-30, assuming 300 µg/g H_2O, 8 µg/g Cl and 0.1 µg/g B in PM; Kamenetsky et al., 2010. Composition and temperature of komatiite melts from Gorgona Island constrained from olivine-hosted melt inclusions. Geology 38, 1003–1006). The inclusions range in $\delta^{11}B$ values from −11.5 to +15.6 ± 2.2‰ (1 SE), forming two distinct trends in a $\delta^{11}B$ vs. B-concentration diagram. Direct assimilation of seawater, seawater-derived components, altered oceanic crust or marine sediments by ascending komatiite magma cannot readily account for the volatile contents and B isotope variations. Alternatively, injection of <3% of a ^{11}B enriched fluid to the mantle source could be a plausible explanation for the $\delta^{11}B$ range that also may explain the H_2O, Cl and B excess.

Keywords Komatiites, Gorgona Island, Melt inclusions, Volatile components, Boron isotopes, Ion microprobe

1. Introduction

The Island of Gorgona, Colombia, is a unique place where Phanerozoic komatiites have been first described and then studied in detail (Gansser, 1950; Echeverría, 1980; Aitken and Echeverría, 1984; Echeverría and Aitken, 1986; Kerr et al., 1996; Kerr, 2005; Sinton et al., 1998; Walker et al., 1991, 1999; Révillon et al., 2000, 2002; Serrano et al., 2011). The problem of the origin of Gorgona komatiites is directly connected to the origin of the Caribbean oceanic plateau (also called the Caribbean Large Igneous Province or CLIP; see review by Hastie and Kerr, 2010). The plateau is the remnant of one or more oceanic melting anomalies active during the late Cretaceous in the Pacific realm and represents a large outpouring of mafic volcanism. The main question is whether the mafic volcanic rocks of the Caribbean plateau were erupted onto the Farallon plate and then subsequently transported during the late Cretaceous to the northeast, having collided with a large intra-oceanic arc (i.e., the Great Arc of the Caribbean) or whether formation of the CLIP was related to the opening a large slab window produced by the intersection of the proto-Caribbean spreading ridge with the Great Caribbean Arc (Pindell et al., 2006; Pindell and Kennan, 2009; Hastie and Kerr, 2010 and references therein). Previous age determinations of the Gorgona mafic rocks yielded ages ranging from ~86 to ~92 Ma (Aitken and Echeverría, 1984; Sinton et al., 1998; Walker et al., 1999), more consistent with the first hypothesis where the Galapagos plume head impacted the Farallon plate. However, a recent set of robust ^{40}Ar-^{39}Ar ages (Serrano et al., 2011) obtained for the main types of Gorgona mafic rocks (komatiites, peridotites, gabbros, picritic basalts) documents much longer magmatic activity on the island, spanning from ~99 to ~61 Ma. This data questions, in fact, the broadly accepted model suggesting that the Caribbean Large Igneous Province formed ultimately due to melting of a plume head at ~90 Ma. Furthermore, Serrano et al. (2011) have demonstrated that multiple magmatic pulses over several tens of Ma, which resulted in a long period of diffuse magmatism without a clear pattern of migration recognized as within a small area like Gorgona Island as in other Caribbean LIP areas, can be broadly coeval with the opening of the Caribbean slab window between ~100 and ~66 Ma.

The abundances of volatile components in komatiitic magmas represent a central issue in their origin because the presence of volatiles in the mantle source considerably affect peridotite

87 solidus, shifting it to lower temperature and pressure and thus this information is essential to
88 constrain the thermal and chemical evolution of the deep Earth. The controversy remains as to
89 whether komatiites represent the products of essentially dry and hot melting of the mantle or
90 whether they result from melting of rising wet plumes, which gained their volatiles by slab
91 dehydration during subduction (e.g., Allègre, 1982; Arndt et al., 1997; 1998; Parman et al., 1997;
92 Litasov and Ohtani, 2002; Wilson et al., 2003; Grove and Parman, 2004; Herzberg, 1995;
93 Herzberg et al., 2007; Berry et al., 2008 among others). Although many existing studies are
94 traditionally skeptical about a wet origin of the Archaean komatiites (e.g., Arndt et al., 1998 and
95 references therein), numerous petrological, geochemical and experimental data indicate, for
96 instance, that komatiites from the 3.5 Ga Barberton Greenstone Belt and from 3.3 Ga
97 Commondale, South Africa are hydrous, characterized by somewhat elevated SiO_2 contents,
98 exhibit boninite-like trace element spectra and are believed to have formed due to subduction
99 zone impact (e.g., Wilson et al., 2003; Grove and Parman, 2004). In addition, several recent
100 studies utilizing the melt inclusion approach and focusing on the 2.7-Ga-old Belingwe
101 komatiites, Zimbabwe, have argued that primary komatiitic magmas may contain up to 1 wt.%
102 H_2O, but the source of water appears to be controversial (shallow depth magma contamination
103 versus melting of a hydrous mantle plume source; Shimizu et al., 2001; Berry et al., 2008; Kent
104 et al., 2009).

105 Although melt inclusions in minerals are routinely used to assess temperature, pressure
106 and redox conditions of magma crystallization, chemical composition and the volatile budget of
107 many rock types (e.g., Sobolev and Danyshevsky, 1994; Sobolev and Chaussidon, 1996;
108 Gurenko and Chaussidon, 1995, 1997; Kent et al., 1999; Danyushevsky et al., 2002a; Rose et al.,
109 2001; Gurenko et al., 2005; Le Voyer et al., 2008), the melt inclusion approach has not been
110 widely used to investigate komatiites, apart from a few studies (McDonough and Ireland, 1993;
111 Shimizu et al., 2001; 2009; Danyshevsky et al., 2002b; Berry et al., 2008; Kent et al., 2009;
112 Kamenetsky et al., 2010). In part, this is because (a) komatiites are always intrinsically altered
113 with a significant proportion of their phenocrystic olivine having been fractured and replaced by
114 serpentine, and (b) melt inclusions entrapped during rapid growth of the spinifex olivine often
115 remain connected to groundmass so that their volatile concentrations can be biased by shallow

depth magma degassing. Recently, Shimizu et al. (2009) and Kamenetsky et al. (2010) described volatile-enriched melt inclusions in spinel and olivine from Gorgona komatiitic lavas, with contrasting interpretations. In particular, strong enrichment in volatile elements (CO_2, F, H_2O and Cl) accompanied by high and variable $H_2O/Ce = 307 \pm 198$, $Cl/K_2O = 1.07 \pm 0.52$ ratios (in spinel-hosted melt inclusions) and by exceptionally high H_2O/Ce ratios of 2000–5000 (in olivine-hosted melt inclusions) were assigned to "seawater/brine assimilation" by the magma at upper mantle depth (Shimizu et al., 2009). In contrast, Kamenetsky et al. (2010) suggested the origin of similar volatile-rich olivine-hosted melt inclusions due to partial melting of a wet mantle plume, resulting in a parental komatiitic magma with ~17 wt.% MgO and up to 1.0 wt.% H_2O, whose crystallization occurred at temperatures as low as 1330–1340°C.

Here, we extend our study and report new boron isotope data coupled with volatile and trace element concentrations obtained for a subset of homogenized melt inclusions reported by Kamenetsky et al. (2010). The central purpose of the present work is to shed more light on the origin of the Gorgona komatiitic magmas. These results can be used to better understand the origin of the Caribbean Large Igneous Province as well as that of komatiitic volcanism worldwide.

1.1. Why boron isotopes?

The light lithophile element boron is a very powerful tracer for crust recycling, slab–mantle wedge interaction or shallow depth contamination because boron has no natural redox chemistry and fractionation between the two isotopes of boron is almost entirely controlled by their partitioning between trigonal (near-neutral aqueous fluids preferentially containing ^{11}B) and tetrahedral species (coordination of B in many silicates, which preferentially incorporate ^{10}B) (Palmer et al., 1987, 1992; Palmer and Swihart, 1996; Peacock and Hervig, 1999; Williams et al., 2001; Hervig et al., 2002; Tonarini et al., 2003; Schmidt et al., 2005; Wunder et al., 2005). The surface reservoirs are enriched in boron, from 2 ± 1 μg/g B in the lower continental crust through 10–15 μg/g B in the upper crust to ~100 μg/g B in the altered oceanic crust and marine sediments (Harder, 1978; Truscott et al., 1986; Spivack and Edmond, 1986; Leeman et al., 1992; Ishikawa and Nakamura, 1992, 1993; Smith et al., 1995, 1997;

Kasemann et al., 2001; Savov et al., 2009), as compared to the Earth mantle having 0.05–0.25 μg/g B (Ryan and Langmuir, 1993; Chaussidon and Jambon, 1994; Chaussidon and Marty, 1995).

Boron isotopes significantly fractionate during surface geochemical processes (δ^{11}B expressed relatively to NBS 951 standard range from –30 to +60‰ in natural samples from different geological environments; Palmer and Swihart, 1996). Their fractionation is negligible during high-temperature igneous processes, such as partial melting and fractional crystallization, because (a) boron is an incompatible element and remains mostly in the melt (Chaussidon and Libourel, 1993; Chaussidon and Jambon, 1994) and (b) the isotopic fractionation factor ($\alpha_{trigonal\text{-}tetrahedral} = [^{11}B/^{10}B]_{trigonal}/[^{11}B/^{10}B]_{tetrahedral}$), as first demonstrated by Kotaka (1973) and Kakihana et al. (1977) using the example of $B(OH)_3$ (boric acid) and $[B(OH)_4]^-$ species in the aqueous solutions, decreases strongly from 1.0193 at 300 K to 1.00704 at 700 K but stays nearly constant at higher, magmatic temperatures (1.00393 at 1000 K and 1.00188 at 1500 K). Several "second-order" effects (e.g., differences in geometries and bonding energies between $[BO_4]$-tetrahedra in micas and $[B(OH)_4]^-$ species in fluids, presence of various, chemically different species of boron associated with K, Al, and Si complexes in melts and fluids at high pressures and temperatures) can also play an important role in fractionation of B isotopes (Tonarini et al., 2003; Schmidt et al., 2005; Wunder et al., 2005).

Boron isotopic composition of fresh basalts is variable, ranging from –9.4 ± 4.0‰ in the mafic continental rift lavas through –7.3 ± 4.0‰ in oceanic island basalts (OIB) and –3.3 ± 2.2‰ in mid-ocean ridge basalts (MORB) to –0.8 ± 5.0‰ in back arc basin basalts (BABB) (Chaussidon and Jambon, 1994; Chaussidon and Marty, 1995). Later, strongly negative δ^{11}B values of –7.2‰ in the Central Andes and –17.9‰ in Ecuadorian arc lavas were described by Rosner et al. (2003) and Le Voyer et al. (2008). The δ^{11}B value of –10 ± 2‰ has been estimated for the OIB mantle source, and –4.0 ± 1.6‰ and –3.6 ± 1.9‰ for the N-MORB and E-MORB mantle sources, respectively (Chaussidon and Marty, 1995). However, somewhat higher values inferred for the N- and E-MORB sources obtained on the basis of pillow rim glass compositions were explained by probable interaction of the magmas with oceanic crust. Later, Gurenko and

Chaussidon (1997) demonstrated the overall ^{11}B-depleted signature of the Icelandic mantle (δ^{11}B = –11.3 ± 1.9‰), based on a study of very primitive olivine-hosted melt inclusions.

Systematically higher δ^{11}B values reported for arc lavas compared to exhumed subduction related metamorphic rocks suggest that dehydration reactions significantly decrease the δ^{11}B values of the subducting oceanic crust and sediments, implying strong fractionation of ^{11}B and ^{10}B isotopes as boron partitions in the fluid (Peacock and Hervig, 1999). In particular, this is supported by experimental study of Wunder et al. (2005), which has shown that a wide range of δ^{11}B values in volcanic arcs may result from continuous dehydration of micas. Another major carrier of boron, also a source of variable but generally positive δ^{11}B values, is the serpentinized mantle wedge at the slab-mantle interface (e.g., Benton et al., 2001; Savov et al., 2005, 2007). In relation to these sources of B, the formation of a hydrated wedge due to infiltration of B-rich fluids progressively released from the down dragged slab at arc front depths may account for strongly varying crossarc boron isotopic signatures (Straub and Layne, 2002). On the other hand, Chaussidon and Jambon (1994), Chaussidon and Marty (1995) and Smith et al. (1995) have demonstrated that positive δ^{11}B values accompanied by elevated δ^{18}O of >5.5‰ and increasing radiogenic Sr isotope ratios in primitive MORB and OIB magmas can result from shallow-level assimilation of the oceanic crust, whereas the negative δ^{11}B related with relatively low δ^{18}O values of <5.5‰ can be due to interaction of these magmas with the Layer 3 gabbroic crust (for reference, see oxygen isotope profile through the altered, sediment-covered oceanic crust of the Oman ophiolite; Gregory and Taylor, 1981). Finally, B isotope variations from –8.9 to –0.8‰ in the Snake River Plain–Yellowstone rhyolites can be ascribed to the existence of distinctive sources of boron coming from either juvenile basalt-derived protoliths sitting in the crust or from strongly fluid-depleted, metamorphosed continental crust (Savov et al., 2009). All of the above information suggests that boron isotopes represent a powerful tool which can be effectively used to understand the origin of the Gorgona komatiitic magmas.

2. Geological background and studied samples

Gorgona is a small island (8.3 km long and 2.5 km wide) located approximately 50 km to the west off the Pacific coast of Colombia (**Fig. 1**). The geology of Gorgona was first described

in Gansser (1950) and Echeverría (1980) and interpreted as a sequence of tilted and faulted blocks of mafic and ultramafic rocks surrounding an axial ridge of cumulate peridotites. The central part of the island is an undeformed peridotite–gabbro complex. Basalts are by far the most abundant eruptive rock type. The komatiite lava flows (1.5 to 6 m thick), often having chilled zones ("polyhedrally jointed zones") at their upper margins, are interlayered with basaltic flows and sills (Kerr, 2005; **Fig. S1a, b;** *Supplementary online material*).

The upper polyhedrally jointed layers are usually 20 to 100 cm thick. They contain skeletal olivine microphenocrysts (0.2–0.5 mm) in a very fine grained matrix, grading into a 10 to 40 cm thick layer composed of fine random spinifex-textured skeletal olivine plates, set in a groundmass of “feathery” pyroxenes. The spinifex textured layer consist of hollow elongated olivine crystals forming chains, blebby chains and plates up to 50 cm in length, which may be underlain by a thin layer (up to 30 cm thick) of horizontally-oriented, skeletal olivine plates up to 10 cm long. Some, not all, flows possess a lower olivine cumulate layer. Where cumulate layers do exist, they are generally thin (20–30 cm) and discontinuous, representing no more than 30% of the flow. The cumulate olivine crystals are up to 1 mm in size, have a predominantly skeletal habit, though polyhedral crystals are also present, and are set in the groundmass composed of radiating needles of clinopyroxene, granular olivine, plagioclase laths and Cr-spinel octrahedra (**Fig. S1c;** *Supplementary online material*).

The studied samples were collected from fresh coastal exposures of komatiites on the NE side of the island (**Fig. 1**). Samples GOR94-3/4/17/44 are from the cumulate zone of komatiitic flows, GOR94-28 represents the jointed top of a flow, and GOR94-17 (Punta Trinidad) is from the cumulate zone of a flow having a vesicular zone. The bulk-rock chemical compositions of the studied samples are given in Kamenetsky et al. (2010).

3. Results

Olivine hosted melt inclusions (up to 60 μm) have rounded, elliptic to tubular morphologies and appear as either clear glass with a shrinkage bubble or microcrystalline aggregates with several bubbles (**Fig. S1d, e;** *Supplementary online material*). Some inclusions exhibit a visible rim of olivine crystallized on the walls, suggesting extensive post-entrapment

crystallization. Olivine phenocrysts containing melt inclusions were re-heated and homogenized prior to analysis with electron and ion microprobes (for more detail see *Supplementary online material*). The concentrations of major and trace elements and the volatile contents of heated, quenched to glass and corrected for Fe loss melt inclusions were reported by Kamenetsky et al. (2010). Here we present only the composition of melt inclusions which were analyzed for boron isotopes, including several additional inclusions analyzed for volatile and trace elements (**Table 1**).

The inclusions are characterized by relatively high contents of volatile components (0.18–1.03 wt.% H_2O, 0.052–0.077 wt.% S, 0.022–0.031 wt.% Cl) and boron (0.61–2.02 µg/g B), displaying positive anomalies in the overall depleted, primitive mantle (PM) normalized trace element and REE spectra ($[La/Sm]_n$ = 0.16–0.35; $[H_2O/Nb]_n$ = 8–44; $[Cl/Nb]_n$ = 27–68; $[B/Nb]_n$ = 9–30, assuming 300 µg/g H_2O, 8 µg/g Cl and 0.1 µg/g B in PM as normalizing values). The melt inclusions form a compact field of basaltic composition, range from 13 to 18 wt.% MgO, following the common trend of olivine fractionation and accumulation (Fig 2 in Kamenetsky et al., 2010). All inclusions exhibit a very strong enrichment (ca. 10 to 50 times) in H_2O, Cl and B relatively to other trace elements in the multi-element diagram (**Fig. 2**). Their trace element spectra reflect an overall depleted signature ($[La/Sm]_n$ = 0.16–0.38), corresponding to the field of bulk-rock lava compositions.

The B/K ratios ranging from 0.0019 to 0.0063 are systematically higher than those known for primitive N-MORB (B/K of ~0.001) and OIB (B/K of ~0.0003) melt inclusions, pillow rim glasses and lavas (Ryan and Langmuir, 1993; Chaussidon and Jambon, 1994; Gurenko and Chaussidon, 1997). No clear correlations of H_2O, Cl and B contents with other major, trace end especially fluid-mobile incompatible (such as Ba, K, La, Sr) element concentrations are observed. Similarly, the magnitude of B enrichment does not correlate with H_2O or Cl enrichment. We explain this by the very narrow concentration ranges of trace elements in the studied melt inclusions (in particular, 3.1–4.7 µg/g Ba i.e. 12%, 228–343 µg/g K i.e. 11%, 0.5–0.9 µg/g La i.e.13%, and 73–87 µg/g Sr i.e. 5.5% of the average element concentration), which in fact do not exceed the common analytical errors of SIMS measurements for trace elements (the uncertainty ranges between 10 and 30% of 1RSD = 1 relative standard

deviation; Kamenetsky et al, 2010). In addition, the absence of correlations may be consistent with a serpentinized arc source of B (and H_2O and Cl) in the included melts which represents, as demonstrated by Savov et al. (2007), "large slab inventory depletions of B (~75%), Cs (~25%), As (~15%), Li (~15%), and Sb (~8%); surprisingly low (generally less than 2%) depletions of Rb, Ba, Pb, U, Sr; and no depletions in REE and the high field strength elements (HFSE)" (see discussion below).

The δ^{11}B values of the studied melt inclusions ranging from –11.5 to +15.6 ‰ at B-concentration of 0.6–2 μg/g also show only subtle correlations with some incompatible elements such as K, Sr, Hf and some REEs, if at all. On the other hand, melt inclusions form two distinct trends based on δ^{11}B vs. B relationships (**Fig. 3**). The first trend includes seven of 15 inclusions with relatively low δ^{11}B ranging from –11.5 to –7.3‰ (average –9.0 ± 1.5‰), spanning over the entire range of B concentrations and approaching the "primary" value of the Earth's mantle (–10 ± 2‰; Chaussidon and Marty, 1995). Given that igneous processes such as magma fractionation or partial melting do not cause significant fractionation of boron isotopes, we ascribe this trend to olivine crystallization that may occur either in the magma plumbing system or represent incomplete melting of olivine from the inclusion walls during laboratory experiments. The second trend is characterized by extension of δ^{11}B to highly positive values (up to +15.6‰) with increasing boron concentrations up to 1.6 μg/g B **(Fig. 3)**. Possible reasons of the second trend and its' implications for the origin of Gorgona komatiites are discussed below.

4. Discussion

4.1. Shallow depth magma contamination

A main argument against a hydrous origin of the Gorgona komatiites is their extreme depletion in incompatible trace elements, which progressively increases from basalt through komatiite to picrite, all being related to the same type of the depleted mantle source (e.g., Arndt et al., 1997; Revillon et al., 2000, 2002). In particular, Arndt et al. (1997, p. 297) have noted: "Because the extreme depletion of incompatible elements makes it very unlikely that volatiles were present in the mantle source (they would have been removed along with other incompatible elements during the melt extraction), the parental magma of the tuffs and picrites must have

gained water during passage towards the surface, perhaps through assimilation of hydrated crust in a shallow-level magma chamber". Later, Shimizu et al. (2009) described CO_2-rich (40–4000 µg/g) komatiitic melt inclusions with highly variable H_2O (0.03–0.9 wt.%) and Cl (6–1056 µg/g) contents in Cr-spinels collected in beach sands from Gorgona. They argued that the volatile contents in melt inclusions could be biased prior to their entrapment by magma degassing or interaction with seawater or brine or, alternatively, by possible post-entrapment modification in the inclusions itself. Our first task is therefore to assess whether the compositional signature of the olivine hosted melt inclusions studied during the present work (i.e., varying B isotope composition, positive H_2O, Cl and B anomalies in the incompatible trace element spectra) could result from shallow depth magma contamination.

To answer this question, we examined a two-component mixing scenario, calculating the effects of possible interaction of presumably "uncontaminated" komatiitic magma with seawater, 15%- and 50%-NaCl brine and altered oceanic crust in a similar way as it has been done by Kent et al. (1999) and Shimizu et al. (2009). The isotopic composition of boron together with volatile-to-trace or trace-to-trace element ratios (Cl/K_2O, B/K_2O, H_2O/K_2O), as used by Kent et al. (1999) and Shimizu et al. (2009), were selected for model calculations. Due to the lack of data on the composition of altered oceanic crust, marine sediments and other possible contaminating agents specific to the Gorgona region, most of the end-member compositions represent broad estimates available in the submarine environment. We note that the assigned elemental and isotopic compositions of the selected end-members are fixed values taken from literature, though the number of possible contaminants and their compositional range could be more variable. The employment of the advanced assimilation-fractional crystallization model (e.g., DePaolo, 1981) is not applicable to our particular case because all studied melt inclusions were trapped in Mg-rich olivines of $Fo_{89–91}$, representing very primitive komatiitic magma, which experienced negligible olivine ± Cr-spinel fractionation. Early fractionation of olivine ± spinel cannot significantly affect the volatile contents in the magma since H_2O, Cl, B and K are strongly incompatible in these minerals. Thus, fractionation will cause equivalent enrichment of magma by these elements without affecting their ratios. The following mixing end-members were selected (**Table 2**):

1. "Uncontaminated" komatiitic magma. The concentrations of K (309 µg/g), Ba (4.1 µg/g) and Nb (0.44 µg/g) were defined as average composition of seven ^{11}B-depleted melt inclusions giving average δ^{11}B value of –9.0 ± 1.5‰. The concentrations of H_2O, Cl and B were calculated from the concentrations of neighboring elements of similar incompatibility: $([H_2O]_n = ([La]_n \times [Ce]_n)^{0.5}$, being equal to 0.042 wt.% H_2O, $[Cl]_n = ([Nb]_n \times [K]_n)^{0.5}$, equal to 7.38 µg/g Cl and $[B]_n = ([K]_n \times [La]_n)^{0.5}$, equal to 0.118 µg/g B, so that no enrichment would be visible in the trace element spectra.
2. Seawater. The elemental composition of seawater at 3.5% salinity having 4.5 µg/g B, 19350 µg/g Cl, 392 µg/g K, 0.021 µg/g Ba and 1.5E–05 µg/g Nb was taken from Turekian (1968). Boron isotopic composition (δ^{11}B = +39.5‰) was taken from Leeman and Sisson (1996).
3. 15%- and 50%-NaCl brines. The composition of the brine (15%-NaCl: 85 wt.% H_2O, 99000 µg/g Cl, 2076 µg/g K, 100 µg/g B; 50%-NaCl: 50 wt.% H_2O, 303000 µg/g Cl, 6476 µg/g K) was taken from Kent et al. (1999), who utilized the data of Berndt and Seyfried (1990) obtained for experimental phase-separated brines. The concentrations of Ba = 0.111 µg/g and Nb = 7.94E–05 µg/g in the 15%-NaCl brine and the concentrations of B = 312 µg/g, Ba = 0.347 µg/g and Nb = 2.48E–04 µg/g in the 50%-NaCl brine were calculated by proportional extrapolation of the known concentrations of B in the 15%-NaCl brine given by Kent et al. (1999) and Ba and Nb in seawater to the higher K concentrations by keeping constant their B/K, Ba/K and Nb/K ratios. Boron isotopic composition of natural NaCl brines varies strongly, ranging from +25.5 to +48.7‰ in the brines from the Australian salt lakes and from +55.7 to +57.4‰ in the surface brines of Red Sea, Israel (e.g., Vengosh et al., 1991a, b). We arbitrary assigned the extreme δ^{11}B values of +25.5‰ and +57.4‰ to the 15%- and 50%-NaCl brines, respectively, because, as shown below, such difference in isotopic and trace element composition between 15%- and 50%-NaCl brines only marginally affects the calculation results.
4. Altered oceanic crust (AOC). The chemical composition of AOC, especially that of volatile components, varies strongly between different segments of the ocean floor (e.g.,

Michael and Cornell, 1998). These authors demonstrated that MORBs from the Galapagos spreading center have strongly varying Cl and K concentrations (25–4050 µg/g Cl, 249–4151 µg/g K; Cl/K = 0.06–1.09). For our modeling, we have chosen the concentrations of Cl and K representing mean values of the above ranges (2040 µg/g Cl and 2200 µg/g K, giving Cl/K = 0.93). The concentrations of Ba = 22.6 µg/g, Nb = 1.22 µg/g, H_2O = 5 wt.%, B = 5.2 µg/g and $\delta^{11}B$ = +3.7‰ were taken from Smith et al. (1997), Kent et al. (1999) and Hochstaedter et al. (2001).

5. Siliceous marine sediment (SED). The concentrations of K = 1245 µg/g, H_2O = 8.2 wt.%, Ba = 1950 µg/g, and Nb = 2.44 µg/g correspond to the Colombia sediment from DSDP/ODP drill Hole 504 located 200 km south of the Costa Rica Rift in the eastern equatorial Pacific (Table 1 in Plank and Langmuir, 1998). We note that SED end-member was selected exclusively as one possible, if not a single, end-member to account for the negative $\delta^{11}B$ ratios in ^{11}B-depleted melt inclusions. In contrast to marine carbonates, which are usually characterized by positive and wide range of $\delta^{11}B$ from ~0 to +30‰, the terrigenous, siliceous sediments may have $\delta^{11}B$ as low as −15‰ (Leeman and Sisson, 1996 and references therein). In particular, the concentration of B = 120 µg/g and $\delta^{11}B$ = −10‰ (Smith et al., 1997) were assigned to SED. Although the concentrations of Cl in marine sediments are expected to be strongly varying, we also arbitrary assigned 1000 µg/g Cl to SED because, as stated above, Cl does not play an essential role in our calculations, and the SED mixing lines on the diagrams, except to one panel outlining relationships between $\delta^{11}B$ and B/K_2O, are given only for comparison with other mixing end-members.

As follows from the modeling (**Fig. 4**), direct contamination of the ascending komatiitic magma at shallow depth by crustal rocks, as suggested by Arndt et al. (1997), or by seawater or seawater-derived components (saline brines; Shimizu et al., 2009), is unable to account for the H_2O, Cl and B enrichment observed in the studied melt inclusions. We emphasize that if one would consider mixing relations in coordinates of Cl/K_2O vs. H_2O/K_2O ratios only, following Shimizu et al. (2009), such an approach may lead to an erroneous conclusion. Indeed, to account

for the compositions of melt inclusions with H_2O/K_2O = 4.5–29.6, Cl/K_2O = 0.46–1.04, would require <1.5 wt.% seawater or even <0.7 wt.% of 15%-NaCl brine or <0.2 wt.% of 50%-NaCl brine, respectively (**Fig. 4a**). No effect of AOC or oceanic sediments can be recognized in this diagram. Similarly, mixing the komatiite end-member with 0.5–1.8 wt.% of 15%-NaCl brine or 0.2–0.5 wt.% of 50%-NaCl brine may effectively explain the entire range of B/K_2O ratios found in the studied melt inclusions. In contrast, if we plot the results of this mixing in coordinates of B/K_2O vs. Cl/K_2O (**Fig. 4c**), the essential role of seawater, 15%- and 50%-NaCl brines (the most effective contamination agents in **Fig. 4a, b)**, as well as the role of altered oceanic crust and marine sediments are no longer justified. Mixing relations in coordinates $\delta^{11}B$ vs. B/K_2O (**Fig. 4d**) also provide no evidence for magma contamination. Although admixture of marine sediments (less than 2 wt.% of SED) to the komatiitic magma may potentially account for the $\delta^{11}B$ range in the ^{11}B-depleted melt inclusions, we rule out this possibility because there is no evidence for a significant role of marine sediments from the volatile-trace element relations (**Fig. 4a-c**). In conclusion, we note that our data are also in a good agreement with Walker et al. (1999, p. 722) who have concluded: "Although, the most radiogenic Gorgona komatiites have the lowest Os concentrations in the suite, mass balance arguments weigh heavily against lithospheric contamination of their parental magmas accounting for the enrichments in ^{187}Os".

4.2. Fluid-induced mantle melting: was it due to subduction impact?

Since shallow contamination of the Gorgona komatiitic magmas can not account for volatile enrichment in the melt inclusions, implying a primary juvenile origin of H_2O, Cl and B (Kamenetsky et al., 2010), another process capable of changing B isotopic composition in the included melts, but not major and trace element concentrations, has to be investigated. Relatively high H_2O and Cl abundances in komatiitic melt inclusions have previously been reported for the Belingwe komatiites, Zimbabwe (0.18–0.26 wt.% H_2O, Danyushevsky et al., 2002b; 1.1–1.7 wt.% H_2O, Shimizu et al., 2001; 0.4–0.6 wt.% H_2O, 500–700 µg/g Cl, Cl/K_2O ~0.8–1.5, Kent et al., 2009). In particular, Kent et al. (2009) have suggested generation of the Belingwe komatiitic magmas "from melting of "damp" mantle, possibly with analogies to modern back arc environments".

Although the model proposing that komatiites are generated by dry and hot mantle plumes rising from the thermal boundary layer within the Earth is widely recognized (Arndt et al., 1997; Herzberg, 1995; Kerr, 2005; Kerr et al., 1995, 1996; Walter, 1998; Révillon et al., 2000, 2002; Hastie and Kerr, 2010), an alternative scenario which favors a subduction related origin, recently reviewed in detail by Parman and Grove (2005), apparently could be viable to explain substantial H_2O contents found in several types of komatiites, including those from the Island of Gorgona studied here. As stated above, a recent set of ^{40}Ar-^{39}Ar ages obtained for the main types of Gorgona mafic rocks (Serrano et al., 2011) documents much longer magmatic activity on the island (from 98.7 ± 7.7 to 61.4 ± 4.8 Ma), as compared to the previous age determinations of about 86–92 Ma (Aitken and Echeverría, 1984; Sinton et al., 1998; Walker et al., 1999). Serrano et al. (2011) concluded that the diffuse magmatism occurred in Gorgona Island shows no clear pattern of migration, being broadly coeval with the opening of the Caribbean slab window and question, in fact, the broadly accepted origin of the Caribbean LIP ultimately due to melting of a plume head at ~90Ma. Then, if the model advocated by Serrano et al. (2011) is correct, the fluids released from the subducting slab or from metasomatically reworked mantle wedge might have triggered partial melting in the upwelling mixed mantle, resulting in a wide compositional range of magmas variously enriched or depleted in volatile components and having a range of $\delta^{11}B$ values. This scenario is in agreement with the recent study of Kamenetsky et al. (2010), who also have questioned the ultimately ”hot” signature of the Gorgona komatiites.

A significant fraction of initial boron and ^{11}B isotope inventory is contained in the uppermost few km of the subducting oceanic crust and sediments, being released progressively as subduction proceeds (e.g., Leeman and Sisson, 1996). Boron mobilized from the slab due to its dehydration will be systematically heavier than the parental AOC, resulting in +5 to +10‰ enrichment of the fluid at 400–500°C (Ishikawa and Nakamura, 1992; Leeman and Sisson, 1996; Rose et al. 2001, Rosner et al. 2003; Leeman et al., 2004; Le Voyer et al., 2008). Since the composition of slab-derived fluid may vary strongly, depending closely on the composition of the subducting crust, on one hand, and the degree of its devolatilization, on another, a wide $\delta^{11}B$ range from –7‰ through +2‰ up to +15‰ (assuming +10‰ enrichment of the fluid phase

relative to the upper end of δ^{11}B values given for AOC by Smith et al., 1997) is very probable (Rose et al. 2001; Leeman et al., 2004; Gurenko et al., 2005; Le Voyer et al., 2008; Tonarini et al., 2011 and references therein). The recent study by Tonarini et al. (2011) reports boron isotope data for the South Sandwich Island arc lavas, emphasizing their very positive δ^{11}B values (+12 to +18‰, being the heaviest yet observed for subduction-related rocks), substantial enrichment in B concentrations (3 to 25 µg/g B) and decoupling of B from other fluid-immobile incompatible elements. All these signatures are very similar to what we observe for the Gorgona melt inclusions, except for relatively high B concentrations. The authors propose multi-stage recycling of high-δ^{11}B and high-B serpentinite (mixed with arc crust and sediment material) as a possible source of extremely ^{11}B-rich fluids. Presence of serpentinite in the slab is particularly important because (a) minimal B isotopic fractionation is expected during breakdown of serpentinite minerals, (b) high-δ^{11}B and high-B concentration fluids can be hosted in serpentine minerals up to 3–4 GPa and 650 °C and (c) when released, these fluids may account for decoupling of B and trace elements such as Rb, Ba, Pb, U, Sr (Ulmer and Trommsdorff, 1995; Benton et al., 2001; Savov et al., 2005, 2007; Tonarini et al., 2011).

Similar processes of fluid-enhanced partial melting of a hot mantle plume can be considered to account for the δ^{11}B range in the Gorgona melt inclusions. The effects of possible interaction of slab-derived fluids with depleted MORB-like mantle source are illustrated on diagrams in coordinates of δ^{11}B vs. B/Nb and Ba/Nb ratios (**Fig. 5**). Given that ^{10}B/^{11}B, B/Nb and Ba/Nb ratios do not change significantly during partial melting or magma crystallization processes, the ratios of these elements calculated for the source can be directly applied to the resulting partial melts. The mixing end-members were defined as below (**Table 2**):

1. Mantle (MANT). A depleted trace element and radiogenic isotope signature of the Caribbean plume giving rise to the Gorgona komatiites has been proposed by Arndt et al. (1997). Taking into account the overall trace element depleted composition of the studied melt inclusions, a depleted MORB-like mantle component containing 1.2 µg/g Ba, 0.21 µg/g Nb, 0.06 µg/g B but having δ^{11}B = –10‰ (Chaussidon and Marty, 1995; Salters and Stracke, 2004) has been selected.

2. Recycled crust (REC). The concentrations of trace elements and B in the recycled crust, whose potential presence in the source of the Gorgona komatiites can be deduced from Re-Os isotope systematics (Walker et al., 1991, 1999), was taken to be the same as that of AOC previously used in modeling. The B isotopic composition of REC was fixed at –12.8‰, corresponding to δ^{11}B value of the residual slab (Tonarini et al., 2011).
3. Serpentinite (SERP). The forearc serpentinized peridotites are characterized by a wide range of boron contents (6.6–126 μg/g B), boron isotopic composition (+10.4 to +25.3‰) and trace element concentrations (Benton et al., 2001; Savov et al., 2005, 2007). The presence of a serpentinized mantle wedge at the slab-mantle interface and its admixture into the ascending hot mantle plume may potentially modify the composition of the source rocks whereas the plume penetrates through a gap in the slab. We thus consider serpentinized peridotite as a possible mixing end-member, assigning the following composition: 3.2 μg/g Ba, 0.1 μg/g Nb, 20 μg/g B and δ^{11}B = 14.8‰ based on the data by Benton et al. (2001) and Savov et al. (2005, 2007).
4. Subducting slab fluid (SSF). Three subducting slab fluid compositions (SSF1 through SSF3) with contrasting B concentrations and isotopic compositions (SSF1: 1000 μg/g Ba, 200 μg/g B, δ^{11}B = 15‰; SSF2: 500 μg/g Ba, 100 μg/g B, δ^{11}B = 2‰; SSF3: 250 μg/g Ba, 50 μg/g B, δ^{11}B = –7‰ at constant Nb = 0.36 μg/g) were compiled based on the Rosner et al. (2003), Leeman et al. (2004), Gurenko et al. (2005), Le Voyer et al. (2008) and Tonarini et al. (2011) data. The decrease of B and Ba contents and δ^{11}B values in the fluid components qualitatively reflects the increase of slab temperature and degree of its devolatilization. We note that the fluids released from ultramafic slab ± serpentinite and recycled forearc serpentinites (Tonarini et al., 2011) are within the range of SSF1 to SSF3 compositions currently used and thus not considered as individual end-members.

As follows from the calculations, the major agent affecting the chemical composition of the hybrid mantle source and, consequently, the magmas formed by its partial melting is the composition of a fluid component released from the slab (in the case of subduction related scenario) or the composition of the crust in the magma source (recycling scenario). The presence

of ancient recycled crust in the source region (~10%, depending on the B/Nb or Ba/Nb variables used; **Fig. 5**), is possible but accounts only for a restricted part of the most δ^{11}B-depleted melts. On the other hand, this amount is in a very good agreement with Re-Os isotopic data of Walker et al. (1999), who proposed that only a minor amount (<10%) of the recycled material might be present in the source of Gorgona komatiites. The role of serpentinized peridotites, which may occasionally be entrained by the hot rising plume, is also limited. These may account only for the most δ^{11}B-enriched melts, requiring 1–10% of admixture.

The injection of the slab-derived fluids into melting region appears to be the most effective mechanism, as for producing B isotope variability because there is a wide range of δ^{11}B and B/Nb and Ba/Nb ratios in the fluid phase, as for decreasing the temperature of peridotite solidus. Less than 1 wt.% of SSF1 or SSF2 fluid has to be injected in the ascending hot mantle material in order to explain the observed δ^{11}B enrichment up to ~16‰. The majority of low-δ^{11}B melt inclusions would require admixture of less that 3 wt.% of the SSF3 fluid, representing the most high temperature product of slab devolatilization. We note that such a small amount of this fluid will not result in a significant enrichment in fluid mobile incompatible trace elements, such as Ba, B (both used in calculation), K, La, Ce and Sr, which are typical in subduction-related magmas, and thus may argue for the immediate role of subduction-derived aqueous fluids in the origin of H_2O, Cl and B enrichment. Finally, our data support the conclusion by Kamenetsky et al. (2010) who demonstrated that in the presence of 0.2–1.0 wt.% H_2O in the melt, the initial crystallization temperature of the Gorgona komatiitic magma could be as low as 1330–1340°C, though being still higher than the temperature of common mid-ocean ridge magmas.

5. Conclusions

1. The olivine-hosted melt inclusions from Gorgona komatiites are characterized by a wide range of δ^{11}B values from −11.5 to +15.6 ± 2.2‰ (1 SE), forming two distinct trends as a function of B concentration. The first major trend includes melts with relatively low and constant δ^{11}B values ranging from −11.5 to −7.3‰ (giving an average of −9.0 ± 1.5‰), while the second trend shows a drastic increase of δ^{11}B up to +15.6‰, at similar but varying (0.6–2 μg/g) concentrations of B.

2. Direct assimilation of seawater, seawater-derived components, altered oceanic crust or marine sediments by ascending komatiite magma cannot readily account for the volatile contents and B isotope variations.
3. Injection of the subduction slab fluid into the rising mantle plume in amount of <3 wt.% provides a plausible explanation for the δ^{11}B range, and also may explain the origin of H_2O, Cl and B enrichment of the Gorgona olivine hosted melt inclusions and slightly elevated, as compared to MORB, but still relatively low initial temperatures of the Gorgona komatiite magmas (Kamenetsky et al., 2010).

Acknowledgements

We thank Andrew Kerr for providing the samples, on which this study was based, Alex Sobolev for fruitful discussions, Pete Burnard for useful comments and improving English, while reading the final version of the manuscript. The Museum of Natural History, Washington, DC, kindly provided us with standards for electron microprobe analysis. We thank Adam Kent and Ivan Savov for their thorough reviews and useful criticism that helped us to improve the manuscript. Editorial handling by Richard Carlson is gratefully acknowledged. Financial support to AAG during data acquisition and manuscript preparation was provided by Northeast National Ion Microprobe Facility (Woods Hole Oceanographic Institution, USA) and the Centre de Recherches Pétrographiqueset Géochimiques (France). This research was also supported by the Australian Research Council (Research Fellowship and Discovery grants to VSK). We acknowledge partial support of the Alexander von Humboldt Foundation, Germany (F.W. Bessel Award to VSK and Wolfgang Paul Award to A.V. Sobolev who provided access to the electron microprobe at the Max Planck Institute, Mainz, Germany). This is CRPG contribution number 2141.

References

Allègre, C.J., 1982. Genesis of Archean komatiites in a wet ultramafic subducted plate. In: Arndt, N., Nisbet, E.G. (Eds.) Komatiites. Berlin, Springer-Verlag, 495–500.

Arndt, N.T., Kerr, A.C., Tarney, J., 1997. Dynamic melting in plume heads: The formation of Gorgona komatiites and basalts. Earth Planet. Sci. Lett. 146, 289–301.

Arndt, N., Ginibre, C., Chauvel, C., Albarède, F., Cheadle, M., Herzberg, C., Jenner, G., Lahaye, Y., 1998. Were komatiites wet? Geology 26, 739–742.

Aitken, B.G., Echeverría, L.M., 1984. Petrology and geochemistry of komatiites and tholeiites from Gorgona Island, Colombia. Contrib. Mineral. Petrol. 86, 94–105.

Benton, L.D., Ryan, J.G., Tera, F., 2001. Boron isotope systematics of slab fluids as inferred from a serpentine seamount, Mariana forearc, Earth Planet. Sci. Lett. 187, 273–282.

Berndt, M.E., Seyfried, W.E.J., 1990. Boron, bromine, and other trace elements as clues to the fate of chlorine in mid-ocean ridges. Geochim. Cosmochim. Acta 54, 2235–2245.

Berry, A.J., Danyushevsky, L.V., O'Neill, H.St.C., Newville, M., Sutton, S.R., 2008. Oxidation state of iron in komatiitic melt inclusions indicates hot Archaean mantle. Nature 455, 960–963.

Chaussidon, M., Libourel, G., 1993. Boron partitioning in the upper mantle: An experimental and ion probe study. Geochim. Cosmochim. Acta 57, 5053–5062.

Chaussidon, M., Jambon, A., 1994. Boron content and isotopic composition of oceanic basalts: geochemical and cosmochemical implications. Earth Planet. Sci. Lett. 121, 277–291.

Chaussidon, M., Marty, B., 1995. Primitive boron isotope composition of the mantle. Science, 269, 383–386.

Danyushevsky, L.V., McNeill, A.W., Sobolev, A.V., 2002a. Experimental and petrological studies of melt inclusions in phenocrysts from mantle-derived magmas: an overview of techniques, advantages and complications: Chem. Geol. 183, 5–24.

Danyushevsky, L.V., Gee, M.A.M., Nisbet, E.G., and Cheadle, M.J., 2002b. Olivine-hosted melt inclusions in Belingwe komatiites: Implications for cooling history, parental magma composition and its H_2O content. Geochim. Cosmochim. Acta 66, A168.

575 DePaolo, D.J., 1981. Trace element and isotopic effects of combined wallrock assimilation and
576 fractional crystallization. Earth Planet. Sci. Lett. 53, 189–202.
577 Dixon, J.E., Clague, D.A., Stolper, E.M., 1991. Degassing history of water, sulfur and carbon in
578 submarine lavas from Kilauea volcano, Hawaii. J. Geol. 99, 371–394.
579 Echeverría, L.M., 1980. Tertiary or Mesozoic komatiites from Gorgona island, Colombia: field
580 relations and geochemistry. Contrib. Mineral. Petrol. 73, 253– 266.
581 Echeverría, L.M., Aitken, B.G., 1986. Pyroclastic rocks: Another manifestation of ultramafic
582 volcanism on Gorgona Island, Colombia. Contrib. Mineral. Petrol. 92, 428–436.
583 Gansser, A., 1950. Geological and petrological notes on Gorgona island in relation to north-west
584 S America. Schweiz. Mineral. Petrograph. Mitt. 30, 219– 237.
585 Gregory, R.T., Taylor, H.P., 1981. An oxygen isotope profile in a section of Cretaceous oceanic
586 crust, Samail ophiolite, Oman: evidence for δ^{18}O buffering of the oceans by deep (>5 km)
587 seawater-hydrothermal circulation at mid-ocean ridges. J. Geophys. Res. 86, 2737–2755.
588 Grove, T.L., Parman, S.W., 2004. Thermal evolution of the Earth as recorded by komatiites.
589 Earth Planet. Sci. Lett. 219, 173–187.
590 Gurenko, A.A., Chaussidon, M., 1995. Enriched and depleted primitive melts included in olivine
591 from Icelandic tholeiites: origin by continuous melting of a single mantle column. Geochim.
592 Cosmochim. Acta 59, 2905–2917.
593 Gurenko, A.A., Chaussidon, M., 1997. Boron concentrations and isotopic composition in the
594 Icelandic mantle: evidence from glass inclusions in olivine. Chem. Geol. 135, 21–34.
595 Gurenko, A.A., Trumbull, R.B., Thomas, R., Lindsay J.M., 2005. A melt inclusion record of
596 volatiles, trace elements and Li-B isotope variations in a single magma system from the Plat
597 Pays Volcanic Complex, Dominica, Lesser Antilles. J. Petrol. 46, 2495–2526.
598 Harder, H., 1978. Boron: granitic rocks and related effusives. In: Wedepohl, K.H., (Ed.),
599 Handbook of geochemistry, II-1. Springer Verlag, Berlin, 5E5–5E10.
600 Hastie, A.R., Kerr, A.C., 2010. Mantle plume or slab window?: Physical and geochemical
601 constraints on the origin of the Caribbean oceanic plateau. Earth-Sci. Rev. 98, 283–293.
602 Herzberg, C., 1995. Generation of plume magmas through time: an experimental perspective.
603 Chem. Geol. 126, 1–16.

Herzberg, C., Asimow, P.D., Arndt, N., Niu, Y., Lesher, C.M., Fitton, J.G., Cheadle, M.J., Saunders, A.D., 2007. Temperatures in ambient mantle and plumes: Constraints from basalts, picrites, and komatiites. Geochem. Geophys. Geosyst. 8, DOI:10.1029/2006GC001390.

Hervig, R.L., Moore, G.M., Williams, L.B., Peacock, S.M., Holloway, J.R., Roggensack, K., 2002. Isotopic and elemental partitioning of boron between hydrous fluid and silicate melt. Amer. Mineral. 87, 769– 774.

Hochstaedter, A., Gill, J., Peters, R., Broughton, P., Holden, P., Taylor, B., 2001. Across-arc geochemical trends in the Izu-Bonin arc: Contributions from the subducting slab. Geochem. Geophys. Geosyst. 2, 2000GC000105.

Hofmann, A.W., 1988. Chemical differentiation of the Earth: the relationship between mantle, continental crust and oceanic crust. Earth Planet. Sci. Lett. 90, 297−314.

Ishikawa, T., Nakamura, E., 1992. Boron isotope geochemistry of the oceanic crust from DSDP/ODP hole 504B. Geochim. Cosmochim. Acta 56, 1633–1639.

Ishikawa, T., Nakamura, E., 1993. Boron isotope systematics of marine sediments. Earth Planet. Sci. Lett. 117, 567–580.

Jarosewich, E.J., Nelen, J.A., Norberg, J.A., 1980. Reference samples for electron microprobe analysis. Geostand. Newslett. 4, 43–47.

Kakihana, H., Kotaka, M., Satoh, S., Nomura, M. Okamoto, M, 1977. Fundamental studies on the ion-exchange separation of boron isotopes. Bull. Chem. Soc. Japan 50, 158−163.

Kamenetsky, V.S., Gurenko, A.A., Kerr, A.C., 2010. Composition and temperature of komatiite melts from Gorgona Island constrained from olivine-hosted melt inclusions. Geology 38, 1003–1006.

Kasemann, S., Meixner, A., Rocholl, A., Vennemann, T., Rosner, M., Schmitt, A., Wiedenbeck, M., 2001. Boron and oxygen isotope composition of certified references materials NIST SRM 610/612 and reference materials JB-2 and JR-2. Geostand. Newslett.: J. Geostand. Geoanalys. 25, 405– 416.

631 Kent, A.J.R., Norman, M.D., Hutcheon, I.D., Stolper, E.M., 1999. Assimilation of seawater-
632 derived components in an oceanic volcano: evidence from matrix glasses and glass
633 inclusions from Loihi seamount, Hawaii. Chem. Geol. 156, 299–319.
634 Kent, A.J.R., Hauri, E., Woodhead, J., Hergt, J.M., 2009. Volatile contents of Belingewe
635 komatiites: Mantle volatile contents and the effects of degassing, Geochim. Cosmochim.
636 Acta 73, A640.
637 Kerr, A.C., 2005. La Isla de Gorgona, Colombia: A petrological enigma? Lithos 84, 77–101.
638 Kerr, A.C., Saunders, A.D., Tarney, J., Berry N.H., Hards, V.L., 1995. Depleted mantle plume
639 geochemical signatures: no paradox for plume theories, Geology 23, 843–846.
640 Kerr, A.C., Marriner, G.F., Arndt, N.T., Tarney, J., Nivia, A., Saunders, A.D., Duncan, R.A.,
641 1996. The petrogenesis of Gorgona komatiites, picrites and basalts: new field, petrographic
642 and geochemical constraints. Lithos 37, 245–260.
643 Kotaka, M., 1973. Chromatographic separation of boron and nitrogen isotopes using pure water
644 as eluent. Ph.D. Dissertation, Tokyo Inst. Tech., 163 pp.
645 Leeman, W.P., Sisson, V.B., 1996. Geochemistry of boron and its implications for crustal and
646 mantle processes. In: Grew, E.S., Anovitz, L.M. (Eds.) Boron: Mineralogy, Petrology and
647 Geochemistry. Rev. Mineral., Mineral. Soc. Am., Washington, DC, 33, 645–707.
648 Leeman, W.P., Sisson, V.P., Reid, M.R., 1992. Boron geochemistry of the lower crust: Evidence
649 from granulite terranes and deep crustal xenoliths. Geochim. Cosmochim. Acta 56,
650 775–788.
651 Leeman, W.P., Tonarini, S., Chan, L.H., Borg, L.E., 2004. Boron and lithium isotopic variations
652 in a hot subduction zone—the southern Washington Cascades. Chem. Geol. 212, 101−124.
653 Le Voyer, M., Rose-Koga, E.F., Laubier, M., Schiano, P., 2008. Petrogenesis of arc lavas from
654 the Rucu Pichincha and Pan de Azucar volcanoes (Ecuadorian arc): Major, trace element,
655 and boron isotope evidences from olivine-hosted melt inclusions. Geochem. Geophys.
656 Geosyst. 9, DOI:12010.11029/12008GC002173.
657 Litasov, K., Ohtani, E., 2002. Phase relations and melt compositions in CMAS-pyrolite-H_2O
658 system up to 25 GPa. Phys. Earth Planet. Inter. 134, 105–127.

McDonough, W.F., Ireland, T.R., 1993. Intraplate origin of komatiites inferred from trace elements in glass inclusions: Nature 365, 432–434.

Michael, P.J., Cornell, W.C., 1998. Influence of spreading rate and magma supply on crystallization and assimilation beneath mid-ocean ridges: Evidence from chlorine and major element chemistry of mid-ocean ridge basalts. J. Geophys. Res. 103, 18325–18356.

Palmer, M.R., Swihart, G.H., 1996. Boron isotope geochemistry: an overview. In: Grew, E.S., Anovitz, L.M. (Eds.), Boron: Mineralogy, Petrology and Geochemistry. Rev. Mineral., Mineral. Soc. Am., Washington, D.C., 33, 709−744.

Palmer, M.R., Spivack, A.J., Edmond, J.M., 1987. Temperature and pH controls over isotopic fractionation during adsorption of boron on marine clay. Geochim. Cosmochim. Acta 51, 2319–2323.

Palmer, M.R., London, D., Morgan VI, G.B., Babb, H.A., 1992. Experimental determination of fractionation of $^{11}B/^{10}B$ between tourmaline and aqueous vapor: a temperature- and pressure-dependent isotopic system. Chem. Geol. 101, 123– 129.

Parman, S.W., Grove, T.L., 2005. Komatiites in the plume debate. In: Foulger, G.R., Natland, J.H., Presnallm D.C., Anderson, D.L. (Eds.), Plates, Plumes, and Paradigms, GSA Special. Publ. 388, 249–256.

Parman, S.W., Dann, J.C., Grove, T.L., de Wit, M.J., 1997. Emplacement conditions of komatiite magmas from the 3.49 Ga Komati Formation, Barberton Greenstone Belt. South Africa Earth Planet. Sci. Lett. 150, 303–324.

Peacock, S.M., Hervig, R.L., 1999. Boron isotopic composition of subduction-zone metamorphic rocks. Chem. Geol. 160, 281– 290.

Pindell, J.L., Kennan, L., 2009. Tectonic evolution of the Gulf of Mexico, Caribbean and northern South America in the mantle reference frame: an update. In: James, K., Lorente, M.A., Pindell, J. (Eds.), The geology and evolution of the region between North and South America. Geol. Soc. London, Special. Publ. 328, 1–55.

Pindell, J.L., Kennan, L., Stanek, K.P., Maresch, W.V., Draper, G.G., 2006. Foundations of Gulf of Mexico and Caribbean evolution: Eight controversies resolved. Acta Geologica 4, 303–341.

688 Plank, T., Langmuir, C.H., 1998. The chemical composition of subducting sediment and its
689 consequences for the crust and mantle. Chem. Geol. 145, 325−394.
690 Révillon, S., Arndt, N.T., Chauvel, C., Hallot, E., 2000. Geochemical study of ultramafic
691 volcanic and plutonic rocks from Gorgona Island, Colombia: The plumbing system of an
692 oceanic plateau. J. Petrol. 41, 1127−1153.
693 Révillon, S., Chauvel, C., Arndt, N.T., Pik, R., Martineau, F., Fourcade, S., Marty, B., 2002.
694 Heterogeneity of the Caribbean plateau mantle source: Sr, O and He isotopic compositions
695 of olivine and clinopyroxene from Gorgona Island. Earth Planet. Sci. Lett. 205, 91−106.
696 Rose, E.F., Shimizu, N., Layne, G.D., Grove, T.L., 2001. Melt production beneath Mt. Shasta
697 from boron data in primitive melt inclusions. Science 293, 281−283.
698 Rosner, M., Erzinger, J., Franz, G., Trumbull, R.B., 2003. Slab-derived boron isotope signatures
699 in arc volcanic rocks from the Central Andes and evidence for boron isotope fractionation
700 during progressive slab dehydration. Geochem. Geophys. Geosyst. 4,
701 DOI:0.1029/2002GC000438.
702 Ryan, J.G., Langmuir, C.H., 1993. The systematics of boron abundances in young volcanic
703 rocks. Geochim. Cosmochim. Acta 57, 1489−1498.
704 Salters, V.J.M., Stracke, A., 2004. Composition of the depleted mantle. Geochem. Geophys.
705 Geosyst. 5, DOI:10.1029/2003GC000597.
706 Savov, I.P., Ryan, J.G, D'Antonio, M., Kelley, K., Mattie, P., 2005. Geochemistry of
707 serpentinized peridotites from the Mariana Forearc- Conical Seamount, ODP Leg 125:
708 Implications for the elemental recycling at subduction zones. Geochem. Geophys. Geosyst.
709 6, Q04J15, doi:10.1029/2004GC000777.
710 Savov, I.P., Ryan, J.G., D'Antonio, M., Fryer, P., 2007. Shallow slab fluid release across and
711 along the Mariana arc-basin system: Insights from geochemistry of serpentinized peridotites
712 from the Mariana Forearc. J. Geophys. Res. 112, doi:10.1029/2006JB004749.
713 Savov, I.P., Leeman, W.P., Lee, C.T., Shirey, S.B., 2009. Boron isotopic variations in NW USA
714 rhyolites: Yellowstone, Snake River Plain, Eastern Oregon. J. Volcanol. Geotherm. Res.
715 188, 162−172.

716 Schmidt, C., Thomas, R., Heinrich, W., 2005. Boron speciation in aqueous fluids at 22 to 600 °C
717 and 0.1 MPa to 2 GPa. Geochim. Cosmochim. Acta 69, 275– 281.
718 Serrano, L., Ferrari, L., Martínez, M.L., Petrone, C.M., Jaramillo, C., 2011. An integrative
719 geologic, geochronologic and geochemical study of Gorgona Island, Colombia: Implications
720 for the formation of the Caribbean Large Igneous Province. Earth Planet. Sci. Lett.,
721 doi:10.1016/j.epsl.2011.07.011.
722 Shimizu, K., Komiya, T., Hirose, K., Shimizu, N., Maruyama, S., 2001. Cr-spinel, an excellent
723 micro-container for retaining primitive melts – implications for a hydrous plume origin for
724 komatiites. Earth Planet. Sci. Lett. 189, 177–188.
725 Shimizu, K., Shimizu, N., Komiya, T., Suzuki, K., Maruyama, S., Tatsumi, Y., 2009. CO_2-rich
726 komatiitic melt inclusions in Cr-spinels within beach sand from Gorgona Island, Colombia.
727 Earth Planet. Sci. Lett. 288, 33–43.
728 Sinton, C.W., Duncan, R.A., Storey, M., Lewis, J., Estrada, J., 1998. An oceanic flood basalt
729 province at the core of the Caribbean plate. Earth Planet. Sci. Lett. 155, 221–235.
730 Smith, H.J., Spivack, A.J., Staudigel, H., Hart, S.R., 1995. The boron isotope composition of
731 altered oceanic crust. Chem. Geol. 126, 119–135.
732 Smith, H.J., Leeman, W.P., Davidson, J., Spivack, A.J., 1997. The B isotopic composition of arc
733 lavas from Martinique, Lesser Antilles. Earth Planet. Sci. Lett. 146, 303–314.
734 Sobolev AV, Danyushevsky LV (1994) Petrology and geochemistry of boninites from the North
735 Termination of the Tonga Trench: Constraints on the generation conditions of primary high-
736 Ca boninite magmas. J Petrol 35: 1183–1211.
737 Sobolev, A.V., Chaussidon, M., 1996. H_2O concentrations in primary melts from supra-
738 subduction zones and mid-ocean ridges: implications for H_2O storage and recycling in the
739 mantle. Earth Planet. Sci. Lett. 137, 45–55.
740 Spivack, A.J., Edmond, J.M., 1986. Determination of boron isotope ratios by thermal ionization
741 mass spectrometry of the dicesium metaborate cation. Anal. Chem. 58, 31–35.
742 Straub, S.M., Layne, G.D., 2002. The systematics of boron isotopes in Izu arc front volcanic
743 rocks. Earth Planet. Sci. Lett. 198, 25–39.

744 Thordarson, T., Self, S., Oskarsson, N., Hulsebosch, T., 1996. Sulfur, chlorine, and fluorine
745 degassing and atmospheric loading by the 1783-1784 AD Laki (Skaftar Fires) eruption in
746 Iceland. Bull. Vol. 58, 205–225.
747 Tonarini, S., Forte, C., Petrini, R., Ferrara, G., 2003. Melt/biotite $^{11}B/^{10}B$ isotopic fractionation
748 and the boron local environment in the structure of volcanic glasses. Geochim. Cosmochim.
749 Acta 67, 1863– 1873.
750 Tonarini, S., Leeman, W.P., Leat, P.T., 2011. Subduction erosion of forearc mantle wedge
751 implicated in the genesis of the South Sandwich Island (SSI) arc: Evidence from boron
752 isotope systematics. Earth Planet. Sci. Lett. 301, 275–284.
753 Truscott, M.G., Shaw, D.M., Cramer, J.J., 1986. Boron abundance and localization in granulites
754 and the lower continental crust. Bull. Soc. Geol. Finl. 58, 169–177.
755 Turekian, K.K., 1968. *Oceans.* Englewood, Cliffs, NJ, Prentice-Hall, 118 pp.
756 Ulmer, P., Trommsdorff, V., 1995. Serpentine stability to mantle depths and subduction-related
757 magmatism. Science 268, 858–861.
758 Vengosh, A., Starinsky, A., Kolodny, Y., Chivas, A.R., 1991a. Boron isotope geochemistry as a
759 tracer for the evolution of brines and associated hot springs from the Dead Sea, Israel.
760 Geochim. Cosmochim. Acta 55, 1689–1695.
761 Vengosh, A., Chivas, A.R., McCulloch, M.T., Starinsky, A., Kolodny, Y., 1991b. Boron isotope
762 geochemistry of Australian salt lakes. Geochim. Cosmochim. Acta 55, 2591–2606.
763 Walker, R.J., Echeverria, L.M., Shirey, S.B., Horan, M.F., 1991. Re-Os isotopic constraints on
764 the origin of volcanic rocks, Gorgona Island, Colombia: Os isotopic evidence for ancient
765 heterogeneities in the mantle. Contrib. Mineral. Petrol. 107, 150–162.
766 Walker, R.J., Storey, M., Kerr, A.C., Tarney, J., Arndt, N.T., 1999. Implications of ^{187}Os
767 isotopic heterogeneities in a mantle plume: evidence from Gorgona Island and Curaçao.
768 Geochim. Cosmochim. Acta 63, 713–728.
769 Walter, M.J., 1998. Melting of garnet peridotite and the origin of komatiite and depleted
770 lithosphere. J. Petrol. 39, 29–60.

771 Williams, L.B., Hervig, R.L., Holloway, J.R., Hutcheon, I., 2001. Boron isotope geochemistry
772 during diagenesis: Part I. Experimental determination of fractionation during illitization of
773 smectite. Geochim. Cosmochim. Acta 65, 1769– 1782.
774 Wilson, A.H., Shirey, S.B., Carlson, R.W., 2003. Archaean ultra-depleted komatiites formed by
775 hydrous melting of cratonic mantle. Nature 423, 858–861.
776 Wunder, B., Meixner, A., Romer, R.L., Wirth, R., Heinrich, W., 2005. The geochemical cycle of
777 boron: Constraints from boron isotope partitioning experiments between mica and fluid.
778 Lithos 84, 206–216.
779
780
781

Figure captions

Fig. 1. Geological sketch map of Gorgona Island (modified after Echeverría,1980; Kerr et al., 1996; Révillon et al., 2000). Sampling locations are marked by sample numbers referred to in the text.

Fig. 2. Multi-element spectra of the olivine-hosted melt inclusions from Gorgona komatiites, demonstrating positive H_2O, Cl and B enrichment relative to other trace and rare earth elements. Concentrations of trace elements in primitive mantle used for normalization are taken from Hofmann (1998); the normalization values for boron, chlorine and water are 0.3 µg/g B, 17 µg/g Cl and 300 µg/g H_2O, as in Kamenetsky et al. (2010). Shaded field represents the composition of Gorgona picrites, komatiites and D-basalts from Kerr et al. (1996), Arndt et al. (1997), Révillon et al. (2000) and Serrano et al. (2011).

Fig. 3. Boron contents and isotopic composition of the olivine-hosted melt inclusions from Gorgona komatiites. Bars represent ±1 SE analytical precision, shown individually for each B isotope measurement (Y axis) and corresponding to the average ±10% analytical precision in the case of B concentration. The box labeled *Mantle* represents the range of OIB mantle source ($\delta^{11}B = -10 \pm 2‰$ at 0.05–0.25 µg/g B), as suggested by Ryan and Langmuir (1993), Chaussidon and Jambon (1994), Chaussidon and Marty (1995). Dashed arrows visually emphasize two possible trends of magma evolution: (1) the increase of B concentration at nearly constant boron isotopic composition that may be ascribed to high temperature olivine crystallization, and (2) concurrent increase of B concentration and $\delta^{11}B$ values that may result either from magma contamination at shallow depth or from interaction of B-rich subduction-related fluid with mantle source rocks (see discussion).

Fig. 4. Diagrams of (A) Cl/K_2O vs. H_2O/K_2O, (B) B/K_2O vs. H_2O/K_2O, (C) Cl/K_2O vs. B/K_2O and (D) $\delta^{11}B$ vs. B/K_2O (given as weight ratios, except for $\delta^{11}B$ given in ‰) illustrate the effects of addition of different types of contamination products to presumably “uncontaminated” Gorgona komatiitic magma. Mixing lines between presumably “uncontaminated” komatiitic

magma (*KOM*) and seawater (*SW*), 15%- and 50%-NaCl saline brines (labeled *15%-NaCl* and *50%-NaCl*, respectively), altered oceanic crust (*AOC*) and siliceous marine sediment (*SED*) calculated from the compositions given in **Table 2** are shown (see text for explanation). Numbers on mixing lines refer to wt% of component added to parent komatiite. Note that mixing lines calculated for 15%- and 50% NaCl brine end-members almost completely overlap between each other in Panel C. The calculated mixing trends allow us to conclude that direct contamination of the Gorgona komatiitic magmas by altered basaltic rocks at shallow depth, as suggested by Arndt et al. (1997), or by seawater or seawater-derived components (saline brine), as discussed in Shimizu et al. (2009), are unable to account for the H_2O, Cl and B enrichment observed in the melt inclusions studied.

Fig. 5. Diagrams of (A) δ^{11}B vs. B/Nb and (B) δ^{11}B vs. Ba/Nb summarize the proposed interpretation of B-isotope variations in olivine-hosted melt inclusions from the Gorgona komatiites. Mixing lines between the depleted MORB-type mantle (MANT), recycled crust (REC), serpentinized peridotite (SERP) and subduction slab fluids (SSF1, SSF2 and SSF3) are shown. Numbers on mixing lines refer to wt% of component added to MANT end-member.

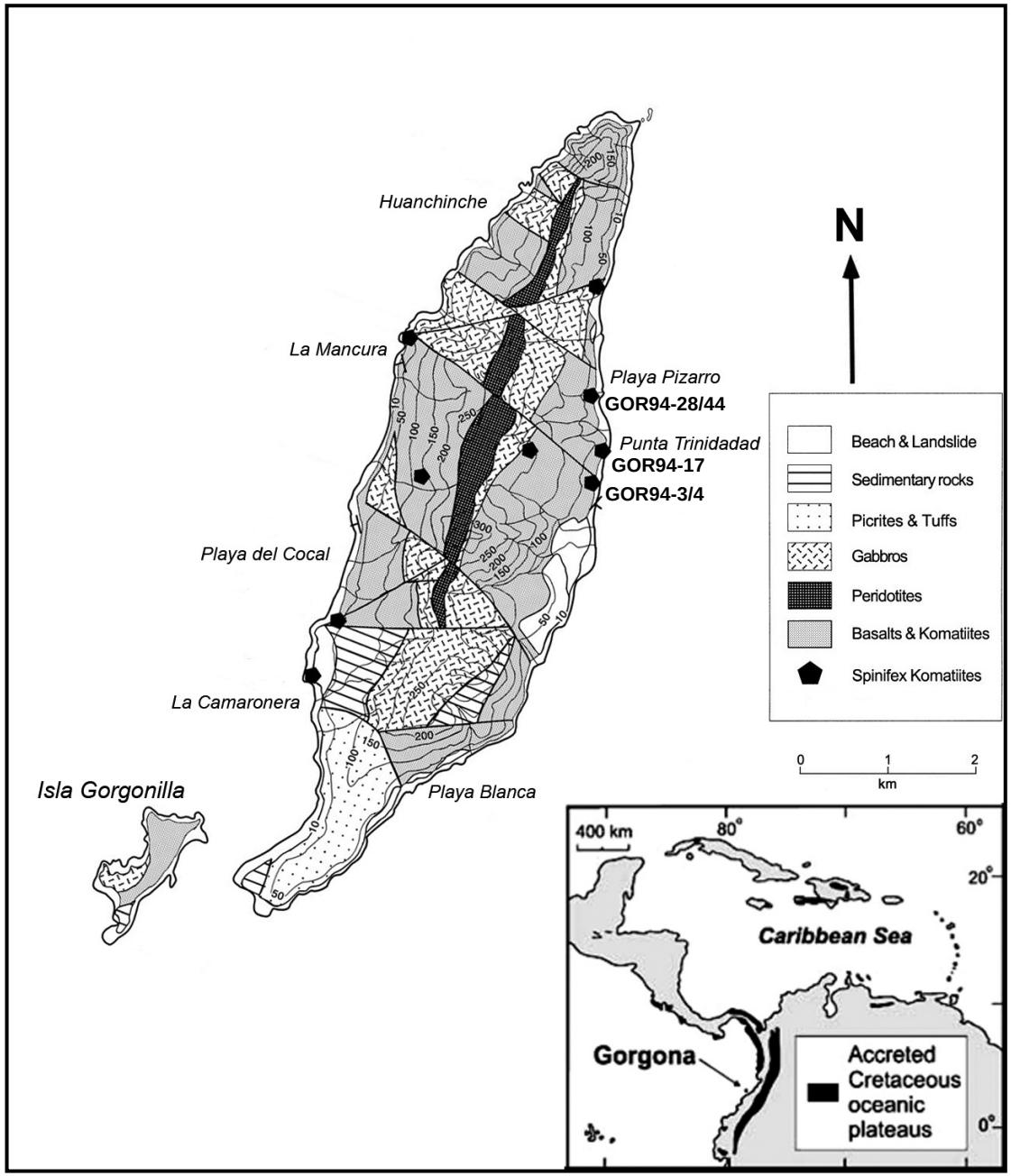

Fig. 1. Gurenko and Kamenetsky

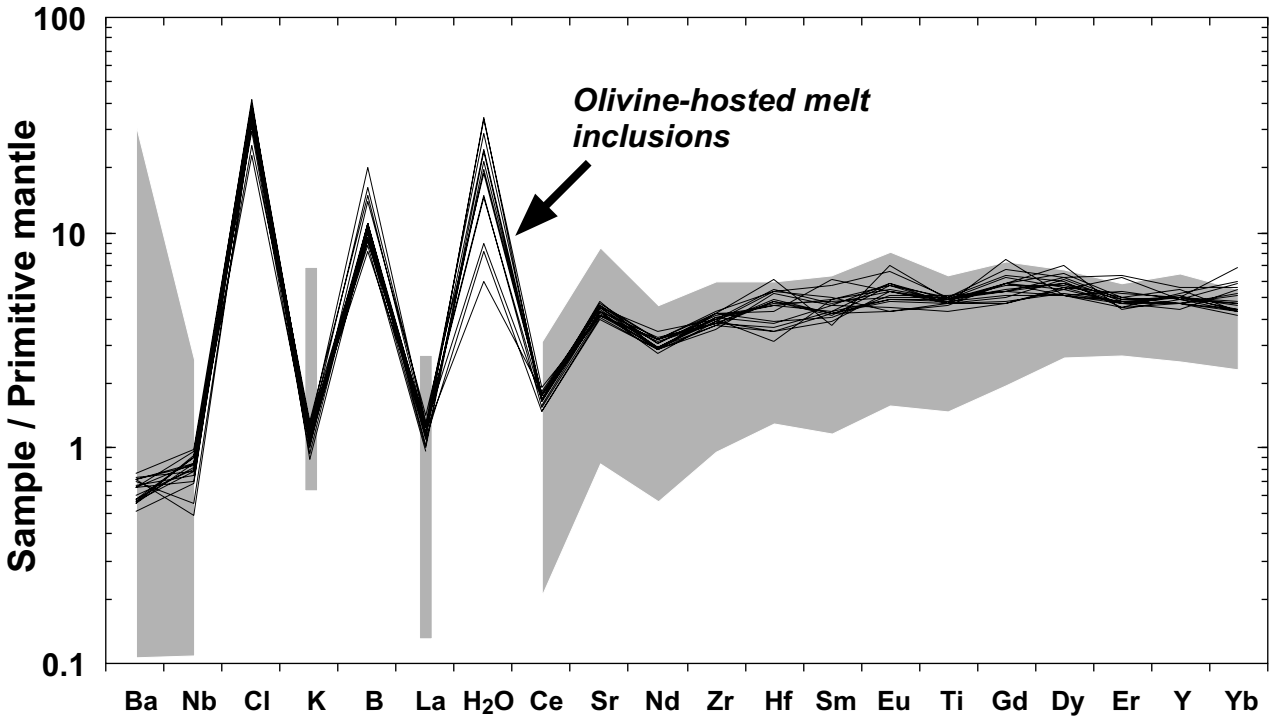

Fig. 2. Gurenko d Kamenetsky

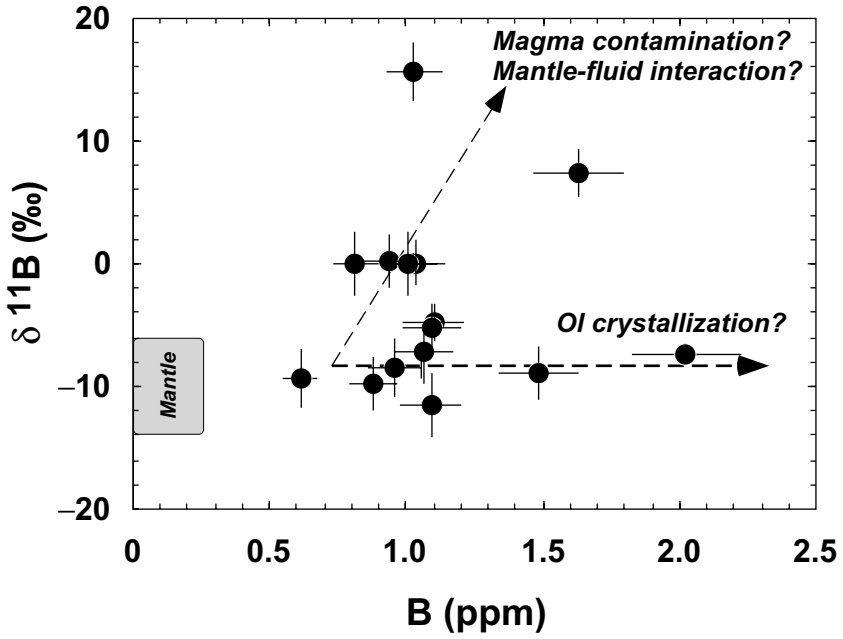

Fig. 3. Gurenko and Kamenetsky

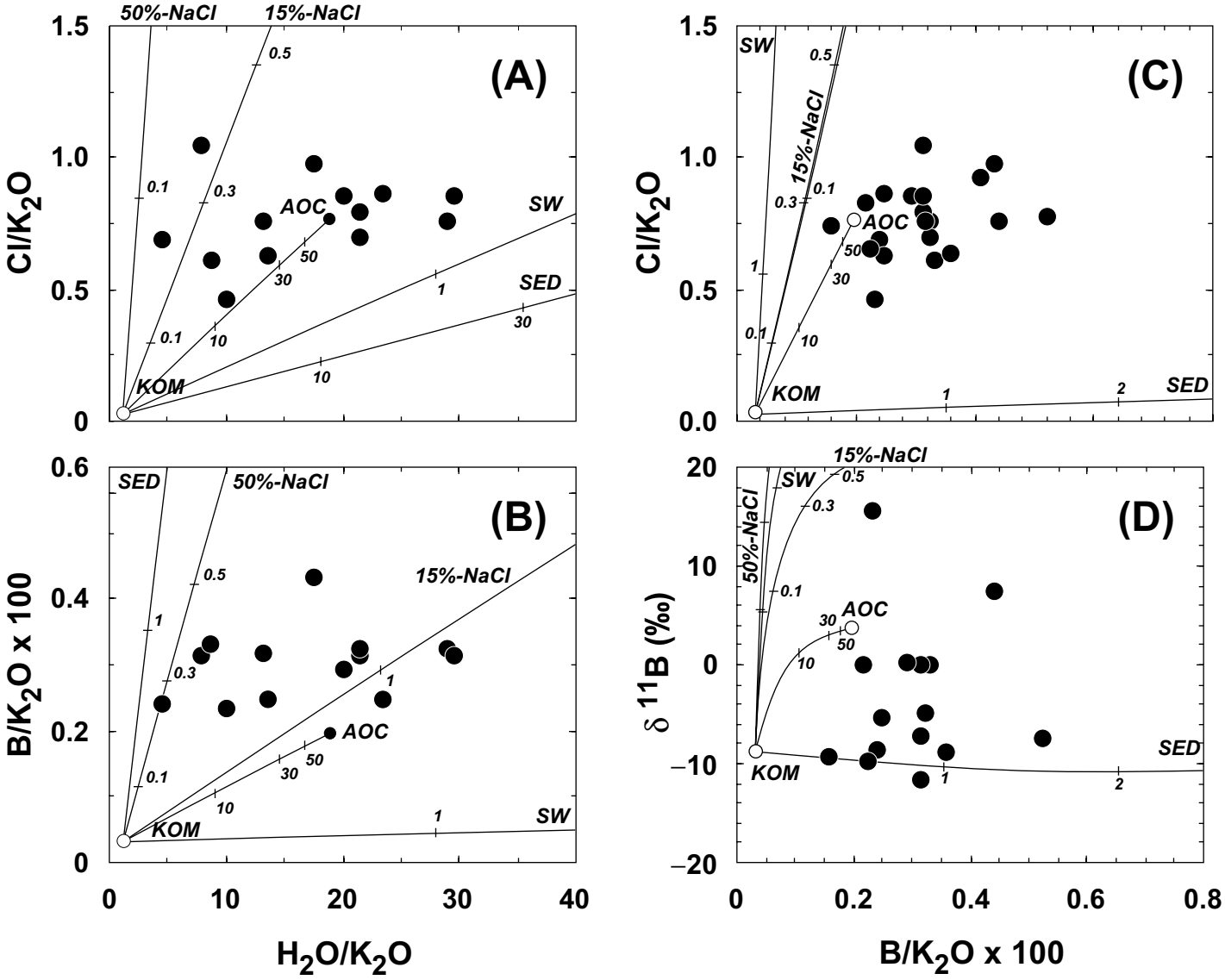

Fig. 4. Gurenko and Kamenetsky

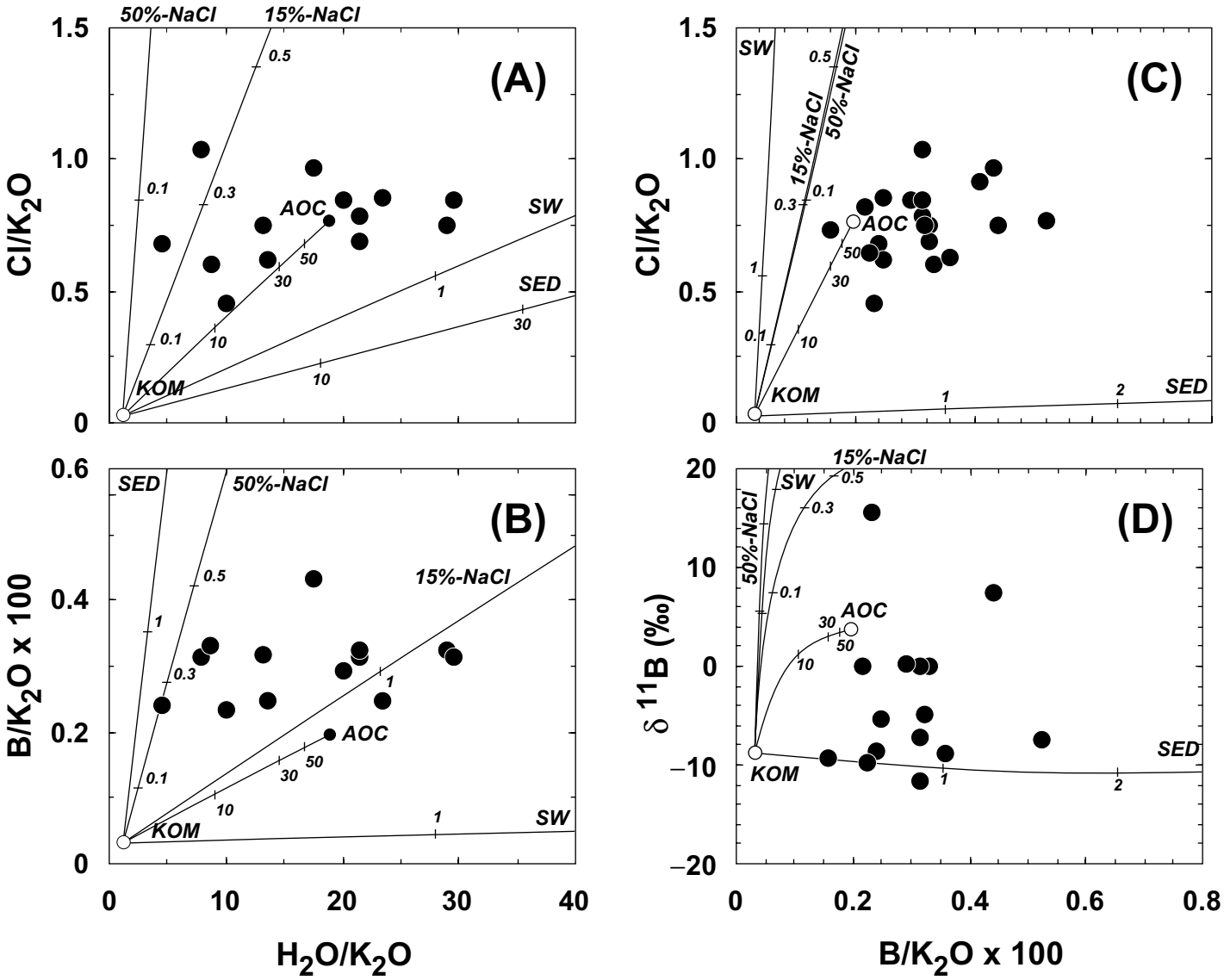

Fig. 4. Gurenko and Kamenetsky

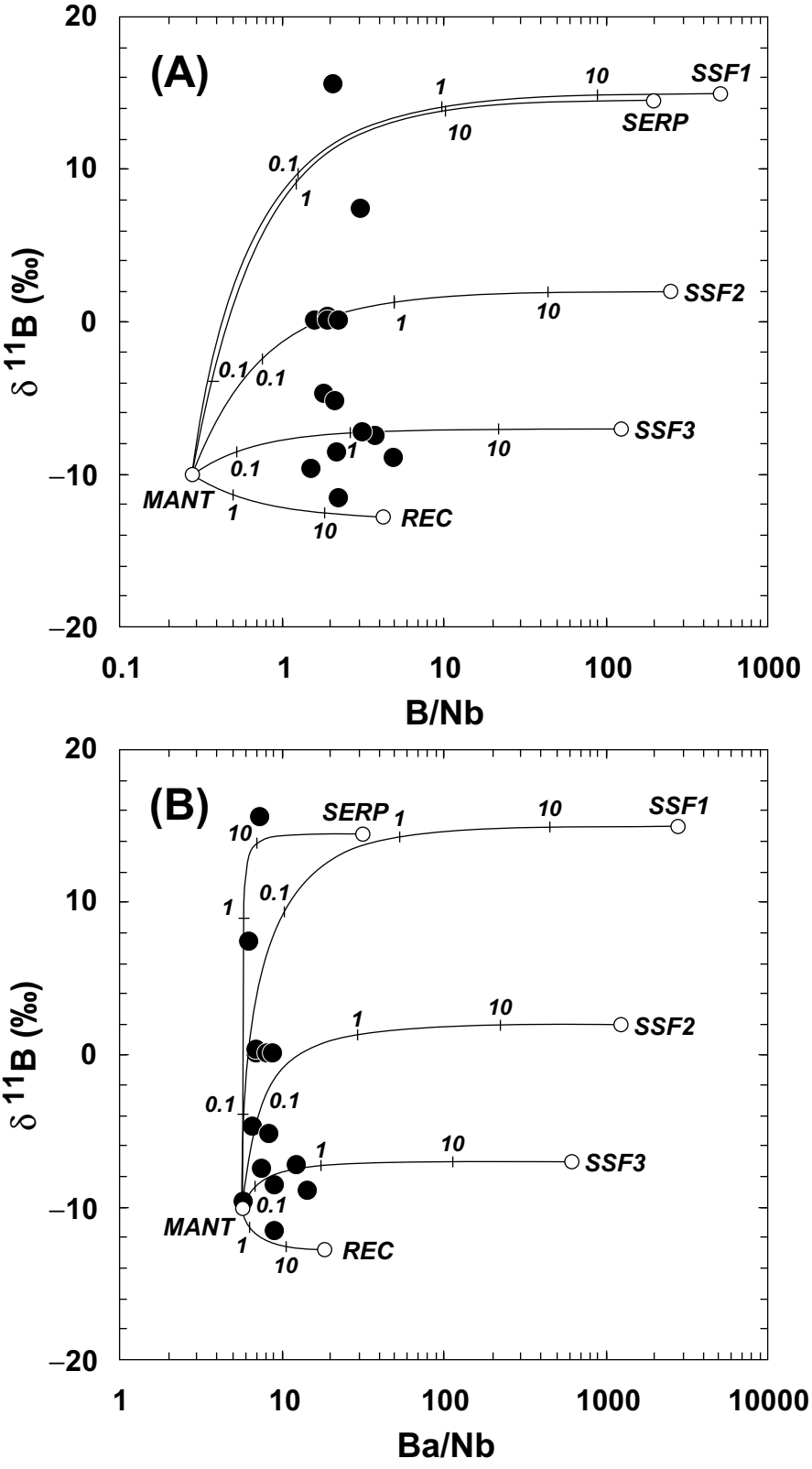

Fig. 5. Gurenke and Kamenetsky

Table 1.
Compositions of the laboratory heated melt inclusions in olivine from Gorgona komatiites, Colombia

Grain No	94-3-30a	94-3-32	94-3-33	94-4-20	94-4-21	94-17-10a	94-17-11	94-17-13	94-17-14	94-17-15	94-17-16	94-28-1	94-28-2	94-28-3a	94-28-7	94-28-8a	94-28-9	94-28-36	94-44-24	94-44-27
Sample	GOR94-3			GOR94-4		GOR94-17						GOR94-28							GOR94-44	
Heated melt inclusions [a]																				
SiO_2	48.25	48.43	48.64	49.02	49.16	48.92	48.61	48.14	48.05	48.59	49.11	49.42	47.98	48.55	48.20	48.84	48.37	47.94	48.94	49.08
TiO2	0.85	0.85	0.83	0.85	0.87	0.85	0.87	0.86	0.88	0.84	0.84	0.95	0.88	0.86	0.88	0.88	0.87	0.86	0.87	0.85
Al_2O_3	15.90	15.85	15.54	15.58	15.91	15.75	15.68	15.60	15.94	15.50	15.46	17.17	16.11	16.12	16.58	16.01	15.79	15.85	15.27	15.50
FeO	6.14	6.91	6.38	6.48	6.23	6.71	6.62	7.11	6.79	7.34	7.57	7.15	7.94	8.37	7.54	8.40	8.90	8.24	6.57	6.56
MnO	0.13	0.13	0.10	0.09	0.09	0.12	0.12	0.15	0.13	0.14	0.15	0.11	0.16	0.18	0.14	0.14	0.13	0.14	0.08	0.11
MgO	11.70	11.45	11.91	11.03	10.76	10.90	10.39	10.76	9.84	10.81	10.95	8.39	9.73	9.92	9.56	9.66	10.06	9.94	10.31	10.43
CaO	13.64	13.75	13.40	13.89	14.17	14.22	14.36	13.88	14.54	13.84	13.79	15.00	14.62	14.07	14.46	14.37	14.13	14.12	14.07	13.95
Na_2O	1.92	1.95	1.89	1.80	1.85	1.83	1.79	1.93	1.92	1.88	1.84	2.12	1.96	1.98	2.06	1.88	1.85	1.89	1.79	1.79
K_2O	0.044	0.030	0.033	0.035	0.044	0.034	0.034	0.034	0.032	0.037	0.032	0.039	0.037	0.039	0.033	0.038	0.040	0.032	0.041	0.039
P_2O_5	0.046	0.054	0.055	0.058	0.061	0.062	0.044	0.052	0.047	0.052	0.054	0.070	0.061	0.062	0.067	0.057	0.056	0.065	0.051	0.046
S	0.052	0.068	0.066	0.056	0.056	0.058	0.052	0.056	0.071	0.063	0.064	0.071	0.077	0.073	0.071	0.072	0.076	0.076	0.052	0.059
Cl	0.023	0.025	0.023	0.029	0.025	0.025	0.026	0.025	0.025	0.022	0.022	0.029	0.028	0.030	0.031	0.031	0.029	0.027	0.026	0.026
Total	98.69	99.49	98.87	98.92	99.22	99.39	98.62	98.60	98.17	99.03	99.88	100.52	99.58	100.24	99.51	100.39	100.31	99.09	98.08	98.44
Host olivine																				
SiO_2	40.84	41.02	40.38	40.34	40.28	40.68	40.80	40.74	40.69	40.32	40.42	40.35	41.34	40.66	41.24	40.22	40.40	40.64	40.68	40.69
FeO	8.48	9.18	8.61	9.37	9.03	9.61	9.72	9.54	9.81	10.39	10.08	9.21	9.02	8.90	8.85	8.97	8.95	9.25	8.65	8.88
MnO	0.12	0.15	0.14	0.14	0.16	0.15	0.17	0.13	0.15	0.16	0.17	0.15	0.15	0.15	0.15	0.14	0.14	0.15	0.12	0.14
MgO	49.99	49.71	49.26	48.81	48.88	48.86	49.06	49.19	48.86	48.05	48.36	49.01	50.02	49.48	50.17	48.56	48.91	49.32	49.45	49.44
CaO	0.31	0.34	0.32	0.32	0.32	0.32	0.33	0.33	0.33	0.34	0.34	0.32	0.33	0.32	0.32	0.32	0.32	0.31	0.32	0.31
NiO	0.44	0.45	0.43	0.42	0.44	0.42	0.40	0.41	0.42	0.39	0.40	0.43	0.44	0.44	0.45	0.44	0.43	0.42	0.44	0.44
Cr_2O_3	0.12	0.13	0.12	0.12	0.11	0.11	0.10	0.12	0.10	0.09	0.11	0.11	0.13	0.12	0.12	0.14	0.14	0.10	0.12	0.11
Total	100.31	100.98	99.25	99.52	99.21	100.14	100.57	100.46	100.36	99.74	99.87	99.56	101.43	100.07	101.30	98.79	99.29	100.19	99.78	100.00
Fo	91.3	90.6	91.1	90.3	90.6	90.1	90.0	90.2	89.9	89.2	89.5	90.5	90.8	90.8	91.0	90.6	90.7	90.5	91.1	90.9
Compositions and temperatures of the trapped melts (normalized to 100%) [b]																				
SiO_2	46.4	46.7	46.8	47.3	47.0	47.1	47.1	46.9	46.8	47.4	47.4	46.7	46.2	46.5	46.2	46.7	46.6	46.6	47.2	47.2
TiO_2	0.7	0.7	0.7	0.7	0.7	0.7	0.7	0.7	0.7	0.7	0.7	0.7	0.7	0.7	0.7	0.7	0.7	0.7	0.7	0.7
Al_2O_3	12.7	13.2	12.6	12.9	12.8	13.1	13.1	13.2	13.4	13.6	13.3	13.2	13.0	13.0	13.1	12.9	13.0	13.2	12.1	12.4
Fe_2O_3	1.4	1.4	1.4	1.4	1.4	1.38	1.4	1.4	1.4	1.4	1.4	1.4	1.4	1.4	1.4	1.4	1.4	1.4	1.4	1.4
FeO	9.6	9.6	9.6	9.6	9.6	9.56	9.6	9.6	9.6	9.6	9.6	9.6	9.6	9.6	9.6	9.6	9.6	9.6	9.6	9.6
MnO	0.1	0.1	0.1	0.1	0.1	0.1	0.1	0.1	0.1	0.1	0.1	0.1	0.2	0.2	0.1	0.1	0.1	0.1	0.1	0.1
MgO	16.6	15.3	16.3	14.9	15.4	14.5	14.4	14.6	14.1	13.3	13.8	15.0	15.4	15.6	15.8	15.3	15.4	15.0	16.3	15.9
CaO	10.9	11.4	10.9	11.6	11.4	11.9	12.0	11.8	12.2	12.2	11.9	11.6	11.8	11.4	11.4	11.6	11.7	11.8	11.2	11.2
Na_2O	1.5	1.6	1.5	1.5	1.5	1.5	1.5	1.6	1.6	1.7	1.6	1.6	1.6	1.6	1.6	1.5	1.5	1.6	1.4	1.4
K_2O	0.03	0.03	0.02	0.03	0.03	0.03	0.03	0.03	0.03	0.04	0.03	0.03	0.03	0.03	0.02	0.03	0.03	0.03	0.03	0.03
P_2O_5	0.04	0.04	0.04	0.05	0.05	0.05	0.03	0.04	0.04	0.04	0.04	0.05	0.05	0.05	0.06	0.05	0.05	0.05	0.04	0.04
T_{calc} ^oC	1383	1358	1376	1347	1358	1339	1337	1343	1332	1314	1325	1352	1362	1365	1370	1357	1359	1352	1375	1368
Ol-add	24.0	18.9	21.7	19.4	22.7	18.2	19.1	17.7	19.2	13.0	14.2	27.1	22.8	22.4	25.5	21.9	20.0	19.9	26.2	24.7

Table 1 (*Continued*)

Grain No	94-3-30a	94-3-32	94-3-33	94-4-20	94-4-21	94-17-10a	94-17-11	94-17-13	94-17-14	94-17-15	94-17-16	94-28-1	94-28-2	94-28-3a	94-28-7	94-28-8a	94-28-9	94-28-36	94-44-24	94-44-27
Sample	GOR94-3			GOR94-4		GOR94-17						GOR94-28							GOR94-44	
Boron isotopes, volatiles and trace elements [c]																				
δ^{11}B, ‰	15.6	0.1	0.1	–11.5	–5.3	ND	–4.8	–7.3	ND	ND	0.3	–9.3	7.4	–7.5	ND	0.0	–8.5	ND	–8.9	–9.7
1σ SE	2.4	2.6	1.8	2.7	2.0	ND	1.5	2.6	ND	ND	2.2	2.5	2.0	1.9	ND	2.6	2.3	ND	2.2	2.2
H_2O	0.44	0.27	0.71	1.03	0.59	1.00	0.73	0.44	0.57	0.87	0.64	ND	ND	ND	ND	ND	0.18	0.25	ND	ND
Cl	205	184	262	296	277	260	236	254	315	321	273	285	280	300	305	313	272	330	263	257
B	1.03	1.01	1.04	1.09	1.10	1.1	1.10	1.07	1.4	0.9	0.93	0.61	1.63	2.02	1.4	0.81	0.95	1.0	1.48	0.88
K	334	270	284	299	308	275	246	265	262	313	290	ND	307	321	274	313	288	228	343	327
Ti	5081	5369	5129	5357	5266	5383	5120	5198	5215	5599	5097	ND	5413	5333	5333	5313	5395	4713	5022	5130
V	405	406	406	453	412	484	369	388	378	462	397	ND	ND	ND	ND	ND	435	300	ND	ND
Cr	686	706	825	736	579	ND	751	444	741	716	484	ND	ND	ND	ND	ND	401	778	ND	ND
Sr	77.0	79.2	78.5	82.2	80.2	75.8	75.2	75.0	81.3	84.3	75.0	ND	86.4	83.3	84.9	86.8	82.3	72.7	78.1	73.7
Y	19.8	19.6	18.7	18.6	19.6	20.7	18.4	18.7	20.4	19.5	19.4	ND	22.0	19.9	22.0	21.5	19.4	17.4	19.5	18.3
Zr	37.9	39.1	38.0	38.2	39.2	38.5	36.5	37.0	38.8	41.0	35.7	ND	42.3	40.9	42.0	41.3	40.4	34.2	37.1	35.9
Nb	0.49	0.52	0.46	0.48	0.51	0.56	0.60	0.34	0.42	0.61	0.48	ND	0.53	0.53	0.42	0.50	0.44	0.56	0.30	0.57
Ba	3.67	4.31	4.06	4.46	4.29	3.52	3.98	4.27	3.07	4.65	3.42	ND	3.35	4.00	4.07	3.49	3.94	3.40	4.36	3.37
La	0.77	0.77	0.63	0.69	0.71	0.71	0.77	0.77	0.87	0.80	0.61	ND	0.81	0.79	0.46	0.77	0.73	0.68	0.77	0.59
Ce	2.71	2.70	2.63	2.65	2.87	3.09	2.81	2.47	2.83	2.83	2.80	ND	2.82	2.72	2.35	2.70	2.94	2.35	2.54	2.38
Pr	0.59	0.55	0.51	0.64	0.56	0.69	0.57	0.60	0.64	0.53	0.55	ND	0.67	0.50	0.66	0.51	0.70	0.44	0.52	0.33
Nd	3.52	3.40	3.26	3.46	3.46	3.81	3.84	3.72	4.17	3.80	3.50	ND	3.81	3.61	3.12	3.43	3.61	3.42	3.89	3.45
Sm	1.92	1.68	1.51	1.89	1.80	1.84	1.68	1.62	1.83	1.57	1.64	ND	2.18	1.44	1.79	2.34	1.88	1.77	1.62	1.60
Eu	0.63	0.71	0.77	0.80	0.85	0.73	0.84	0.72	0.77	0.75	0.69	ND	0.96	1.03	0.60	0.78	0.83	0.65	0.62	0.82
Gd	2.46	3.15	2.96	2.74	2.77	3.23	2.55	2.61	2.97	2.74	2.41	ND	3.44	2.93	2.41	2.98	2.76	2.43	2.95	3.85
Tb	0.51	0.59	0.58	0.51	0.56	0.55	0.52	0.51	0.51	0.57	0.56	ND	0.64	0.59	0.51	0.54	0.56	0.54	0.49	0.44
Dy	3.33	3.52	3.29	3.67	3.71	3.81	3.89	3.28	3.46	3.95	3.47	ND	3.96	3.64	3.57	4.09	3.29	3.55	4.47	3.30
Ho	0.67	0.66	0.71	0.74	0.74	0.84	0.62	0.63	0.59	0.71	0.75	ND	0.81	0.75	0.84	0.91	0.78	0.69	0.65	0.53
Er	2.00	2.16	1.94	2.08	1.98	1.86	2.01	1.89	1.97	2.05	2.61	ND	2.64	2.05	2.00	2.09	2.20	1.94	1.85	2.00
Tm	0.25	0.24	0.29	0.30	0.25	0.27	0.25	0.30	0.27	0.25	0.33	ND	0.34	0.29	0.25	0.32	0.29	0.24	0.38	0.28
Yb	1.83	1.98	2.15	1.83	1.92	2.49	2.10	1.72	1.80	1.96	2.40	ND	2.29	2.88	2.76	1.80	1.94	2.24	1.79	1.79
Lu	0.26	0.28	0.32	0.31	0.35	0.30	0.26	0.23	0.27	0.32	0.32	ND	0.31	0.28	0.24	0.30	0.30	0.30	0.22	0.28
Hf	1.43	1.22	0.94	0.84	1.02	1.25	0.98	1.28	1.46	1.03	0.93	ND	1.44	1.63	1.53	1.16	1.24	1.40	1.31	1.27
Pb	0.40	0.16	0.06	0.11	ND	0.30	ND	0.59	0.71	0.37	0.36	ND	0.10	0.20	0.30	0.09	0.12	0.38	ND	0.05
Th	ND	0.02	0.02	0.02	0.01	0.06	0.02	0.04	0.03	0.03	ND	ND	0.03	0.03	ND	0.02	0.03	0.02	ND	0.02
B/K	0.0031	0.0037	0.0037	0.0036	0.0036	0.0040	0.0045	0.0040	0.0053	0.0029	0.0032	0.0019	0.0053	0.0063	0.0049	0.0026	0.0033	0.0043	0.0043	0.0027
$[La/Sm]_n$	0.25	0.29	0.26	0.23	0.25	0.24	0.29	0.30	0.30	0.32	0.24	–	0.23	0.35	0.16	0.21	0.24	0.24	0.30	0.23
$[H_2O/Nb]_n$	19	10	32	44	24	37	25	27	28	29	28	–	–	–	–	–	8	9	–	–
$[Cl/Nb]_n$	32	27	44	47	42	36	31	58	57	41	44	–	41	44	56	48	48	46	68	35
$[B/Nb]_n$	13	12	14	14	13	12	11	19	20	9	12	–	19	24	20	10	14	11	30	10

Notes for Table 1.

[a] Major element concentrations of the laboratory heated melt inclusions and their host olivines (given in wt%) were analyzed using the JEOL JXA-8200 electron microprobe at the Max Planck Institute for Chemistry (Mainz, Germany) at standard conditions (Kamenetsky et al., 2010). A set of reference materials (i.e. natural and synthetic oxides, minerals and glasses; Micro-Analysis Consultants Ltd, Cambridgeshire, UK) and the Smithsonian Institution standard set for electron microprobe analysis (Jarosewich et al., 1980) were used for routine calibration and instrument stability monitoring. Typical analytical uncertainties (2RSD = 2σ relative standard deviation) are 1.5−3.0% for SiO_2, Al_2O_3, FeO, MgO, CaO, TiO_2; 4–6% for Na_2O, 10% for K_2O, 15% for P_2O_5, and 30% for MnO. As a monitor sample for S and Cl measurements, we also used the USNM 111240/52 VG-2 basaltic glass (recommended values of 0.134−0.137 wt.% S; 0.030 wt.% Cl; Dixon et al., 1991; Thordarson et al., 1996; N. Metrich, personal communication, 2003). The concentrations of 0.140 ± 0.023 wt.% S and 0.029 ± 0.007 wt.% Cl (±2σ SD = 2-sigma standard deviation, N = 37) were obtained during this study (for more detail see Kamenetsky et al., 2010). Fo = mol% of forsterite component of the host olivine.

[b] Calculated compositions and temperatures of the trapped komatiitic melts are based on the compositions of the laboratory heated melt inclusions, corrected for "Fe-loss" and post-entrapment crystallization of host mineral (for detail see Kamenetsky et al., 2010); Ol-add = total amount of olivine (wt%) "added" to the included melts during correction.

[c] Boron isotope composition (in permil units) calculated relative to the NBS 951 standard ($^{11}B/^{10}B$ = 4.04558 ± 0.00033; Spivack and Edmond, 1986) given at ±1σ SE analytical precision (see text for detail). The contents of volatile components (H_2O given in wt%, Cl in µg/g) and trace element concentrations (given in µg/g) were analyzed using the CAMECA IMS 3f ion microprobe and the single collector sector-field ICP-MS Element 2 instrument equipped with the New Wave Research UP213 Nd-YAG (213 nm) laser, both located in the Max Planck Institute for Chemistry, Mainz, Germany (raw values uncorrected for post-entrapment olivine crystallization in melt inclusions are given; for more detail see Kamenetsky et al., 2010). The $[La/Sm]_n$, $[H_2O/Nb]_n$, $[Cl/Nb]_n$ and $[B/Nb]_n$ are element ratios normalized to primitive mantle (PM; assuming 300 µg/g H_2O, 8 µg/g Cl and 0.1 µg/g B, while Nb concentration of 0.6175 µg/g is taken from Hofmann, 1988). ND = not determined, – = no value.

Table 2.
Compositions of the end-members used for calculation of mixing lines (see text for more details).

Component Unit	B µg/g	δ^{11}B ‰	H_2O wt%	Cl µg/g	K µg/g	Ba µg/g	Nb µg/g
KOM[a]	0.118	–9.0	0.042	7.38	309	4.1	0.44
SW[b]	4.5	+39.5	97.5	19350	392	0.021	1.50E-05
15%-NaCl[c]	100	+25.5	85	99000	2076	0.111	7.94E-05
50%-NaCl[c]	312	+56.6	50	303000	6476	0.347	2.48E-04
AOC[d]	5.2	+3.7	5	2040	2200	22.6	1.22
REC[e]	5.2	–12.8	–	–	–	22.6	1.22
SED[f]	120	–10.0	8.2	1000	1245	1950	2.44
MANT[g]	0.06	–10.0	116	0.51	60	1.2	0.21
SERP[h]	20	+14.5	–	–	–	3.2	0.1
SSF1[i]	200	+15.0	–	–	–	1000	0.36
SSF2[i]	100	+2.0	–	–	–	500	0.36
SSF3[i]	50	–7	–	–	–	250	0.36

[a] KOM = "uncontaminated" komatiitic magma representing average composition of seven, the most ^{11}B-depleted melt inclusions (i.e., 94-28-1, -28-3mi1, -28-9, -4-20, -44-27, -17-13, -44-24; Table 1). The concentrations of H_2O, Cl and B were calculated from the concentrations of neighboring elements of similar incompatibility: $[H_2O]_n = ([La]_n \times [Ce]_n)^{0.5}$, $[Cl]_n = ([Nb]_n \times [K]_n)^{0.5}$ and $[B]_n = ([K]_n \times [La]_n)^{0.5}$.
[b] SW = seawater composition at 3.5% salinity.
[c] 15%- and 50%-NaCl brines.
[d] AOC = altered oceanic crust.
[e] REC = recycled crust.
[f] SED = siliceous marine sediment.
[g] MANT = mantle component of the Gorgona komatiite magma source.
[h] SERP = recycled forearc serpentinite.
[i] SSF1-SSF3 = subducting slab fluids.